AD-A093 355 SOUTHEASTERN CENTER FOR ELECTRICAL ENGINEERING EDUCAT--ETC F/G 15/2
FIELD-EFFECT TRANSISTTORS TO DETECT CHEMICAL WARFARE AGENTS IN --ETC(U)
AUG 80 J JANATA, R J HUBER, R COHEN F33615-78-D-0617

UNCLASSIFIED SAM-TR-80-25 NL

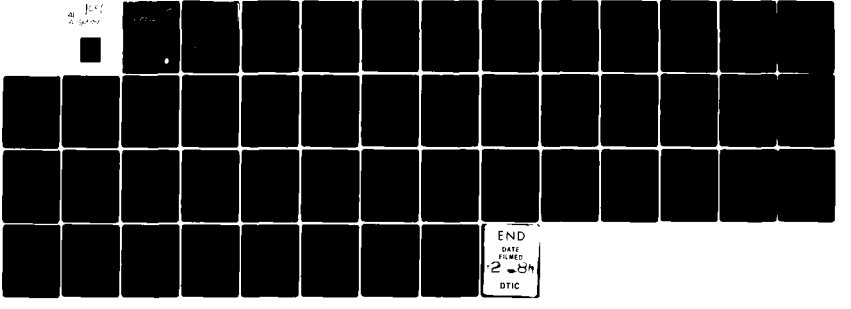

END
DATE FILMED
2-81
DTIC

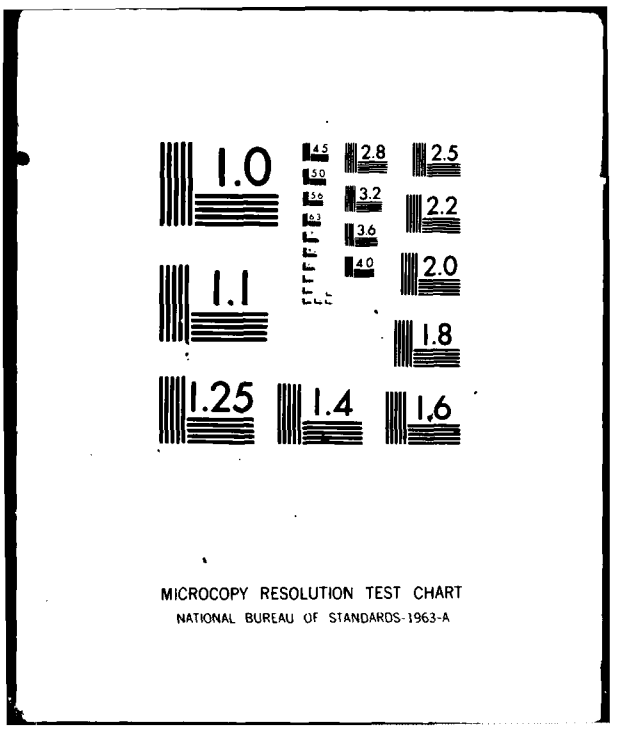
1.0
1.1
1.25
1.4
1.6
1.8
2.0
2.2
2.5
2.8
3.2
3.6
4.0
4.5
5.0
5.6
6.3
MICROCOPY RESOLUTION TEST CHART
NATIONAL BUREAU OF STANDARDS-1963-A

LEVEL II

Report SAM-TR-80-25

AD A093355

FIELD-EFFECT TRANSISTORS TO DETECT CHEMICAL WARFARE AGENTS IN AIRCRAFT

Jiri Janata, Ph.D.
Robert J. Huber, Ph.D.
Richard Cohen, M.S.
Edward S. Kolesar, Jr., Captain, USAF (USAFSAM/VNL)
Department of Bioengineering
University of Utah
Salt Lake City, Utah 84112

DTIC ELECTE DEC 3 1 1980 S D

August 1980

Final Report for Period 31 July 1979 - 30 September 1979

Approved for public release; distribution unlimited.

Prepared for
USAF SCHOOL OF AEROSPACE MEDICINE
Aerospace Medical Division (AFSC)
Brooks Air Force Base, Texas 78235

DDC FILE COPY

80 12 31 030

NOTICES

This final report was submitted by the Department of Bioengineering, University of Utah, Salt Lake City, Utah 84112, under contract F33615-78-D-0617, job order 7930-11-50, with the USAF School of Aerospace Medicine, Aerospace Medical Division, AFSC, Brooks Air Force Base, Texas. Captain Edward S. Kolesar, Jr. (USAFSAM/VNL) was the Laboratory Project Scientist-in-Charge.

When U.S. Government drawings, specifications, or other data are used for any purpose other than a definitely related Government procurement operation, the Government thereby incurs no responsibility nor any obligation whatsoever; and the fact that the Government may have formulated, furnished, or in any way supplied the said drawings, specifications, or other data is not to be regarded by implication or otherwise, as in any manner licensing the holder or any other person or corporation, or conveying any rights or permission to manufacture, use, or sell any patented invention that may in any way be related thereto.

This report has been reviewed by the Office of Public Affairs (PA) and is releasable to the National Technical Information Service (NTIS). At NTIS, it will be available to the general public, including foreign nations.

This technical report has been reviewed and is approved for publication.

Edward S. Kolesar, Jr.

EDWARD S. KOLESAR, JR., Captain, USAF
Project Scientist

RICHARD L. MILLER, Ph.D.
Supervisor

ROY L. DEHART
Colonel, USAF, MC
Commander

UNCLASSIFIED

SECURITY CLASSIFICATION OF THIS PAGE (When Data Entered)

(19) REPORT DOCUMENTATION PAGE	READ INSTRUCTIONS BEFORE COMPLETING FORM
1. REPORT NUMBER (18) SAM-TR-80-25	2. GOVT ACCESSION NO. AD-A093 355	3. RECIPIENT'S CATALOG NUMBER
4. TITLE (and Subtitle) (6) FIELD-EFFECT TRANSISTORS TO DETECT CHEMICAL WARFARE AGENTS IN AIRCRAFT.	5. TYPE OF REPORT & PERIOD COVERED (9) Final Report. 31 Jul 1978-30 Sep 1979
	6. PERFORMING ORG. REPORT NUMBER
7. AUTHOR(s) (10) Jiri Janata, Ph.D.; Robert J. Huber, Ph.D.; Richard Cohen, M.S.; Edward S. Kolesar, Jr., Captain, USAF (USAFSAM/VNL)	8. CONTRACT OR GRANT NUMBER(s) (15) F33615-78-D-0617 Task #23
9. PERFORMING ORGANIZATION NAME AND ADDRESS Department of Bioengineering University of Utah Salt Lake City, Utah 84112 (12) 47	10. PROGRAM ELEMENT, PROJECT, TASK AREA & WORK UNIT NUMBERS 62202F (16) 7930-11-50 (17) 11
11. CONTROLLING OFFICE NAME AND ADDRESS (11) USAF School of Aerospace Medicine (VNL) Aerospace Medical Division (AFSC) Brooks Air Force Base, Texas 78235	12. REPORT DATE August 1980
	13. NUMBER OF PAGES 44
14. MONITORING AGENCY NAME & ADDRESS (if different from Controlling Office)	15. SECURITY CLASS. (of this report) Unclassified
	15a. DECLASSIFICATION/DOWNGRADING SCHEDULE

16. DISTRIBUTION STATEMENT (of this Report)

Approved for public release; distribution unlimited.

17. DISTRIBUTION STATEMENT (of the abstract entered in Block 20, if different from Report)

18. SUPPLEMENTARY NOTES

19. KEY WORDS (Continue on reverse side if necessary and identify by block number)

Chemical field-effect transistor, Chemically sensitive field-effect transistor, CHEMFET, Solid-state gas sensor, Solid-state detector, CSSD, Chemical warfare agent detector, Transistor detectors in chemical warfare, Warfare protection via sensitive transistors, Aircraft with chemical warfare detectors.

20. ABSTRACT (Continue on reverse side if necessary and identify by block number)

Assessed here is the feasibility of utilizing four types of chemically sensitive field-effect transistors (CHEMFETs) as possible candidates for aircraft chemical warfare agent detectors. Analyzed is the integration of chemically sensitive polymers with the field-effect transistor structure. Attention is focused on the design criteria of sensitivity, time response, reversibility, shelf life, operational life, and compactness. Pertinent bibliographic references are included.

DD FORM 1 JAN 73 1473

393 015

UNCLASSIFIED

SECURITY CLASSIFICATION OF THIS PAGE (When Data Entered)

Corporate Source per telecom to Mr. Edward S. Kolesar, Jr., Scientist-in-Charge, School of Aerospace Medicine, Brooks AFB, Texas, 240-2220, Ext. 3362.

JH 2-9-82

C O N T E N T S

	Page
INTRODUCTION	3
GENERAL THEORY OF CHEMICALLY SENSITIVE FIELD-EFFECT TRANSISTORS (CHEMFETs)	4
Metal-Insulator-Semiconductor (MIS) Structure	4
Ideal MIS Structure	4
Current-Voltage Relationships for the Insulated-Gate Field-Effect Transistor (IGFET)	10
Review of Assumptions	19
CHEMFET	19
CHEMFET Sensitive to Neutral Species	20
CHEMFET with Nonpolarized Interface--Ion-Sensitive Field-Effect Transistor (ISFET)	21
TYPES OF CHEMFETS FOR DETECTION OF CHEMICAL WARFARE AGENTS	29
Enzyme-Coupled CHEMFET	29
Feasibility of the Enzyme-Coupled CHEMFET	30
Galvanostatic CHEMFET	30
Feasibility of the Galvanostatic CHEMFET	31
Catalytic CHEMFET	33
Feasibility of the Catalytic CHEMFET	33
Work-Function Dependent CHEMFET	33
Feasibility of the Work-Function Dependent CHEMFET	35
CONCLUSIONS	39
REFERENCES CITED	40
SUPPLEMENTARY REFERENCES	42
ABBREVIATIONS, ACRONYMS, AND SYMBOLS	44

FIGURES

Fig. No.		
1.	Typical metal-insulator-semiconductor structure used to study semiconductor electrical parameters	5
2.	Metal-semiconductor energy-band level under flat-band conditions	6
3.	Metal-semiconductor energy level under bias conditions of interest	7

C O N T E N T S (Cont'd.)

Fig. No.		Page
4.	Cross-section of the n-channel metal-oxide-semiconductor field-effect transistor (MOSFET) structure	11
5.	Cross-section of the field-effect transistor (FET) with small V_G	12
6.	Cross-section of FET channel region with saturated V_G applied	14
7.	Family of I_D vs. V_D curves for a MOSFET	15
8.	I_D vs. V_G curve for depletion mode device	17
9.	I_D vs. V_G curve deviation from ideality due to inherent resistance	18
10.	Response of palladium (Pd)-gate FET to low levels of hydrogen	22
11.	Ion-sensitive FET in solution	23
12.	Cross-section of the ISFET structure shown in Figure 11, as well as the local charge density, electric field, and variations in potential	24
13.	Structure of enzyme-sensitive FET	29
14.	Structure of galvanostatic type of FET	31
15.	I-V curve of the hypothetical electrochemical cell	32
16.	Structure of the catalytic-based FET	34
17.	Structure of the work-function dependent FET	36

FIELD-EFFECT TRANSISTORS TO DETECT CHEMICAL WARFARE AGENTS IN AIRCRAFT

INTRODUCTION

The purpose of this report is to provide a critical assessment of chemically sensitive field-effect transistors (CHEMFETs) as possible detection devices for chemical warfare (CW) agents in the aircraft cockpit. Concurrent work on CW agent binding materials is also taken into consideration (1).

Applicable to this task are four types of CHEMFETs:

a. enzyme-coupled,

b. galvanostatic,

c. catalytic, and

d. work-function.

The operational specifications for the detection system include criteria that will be used to evaluate the feasibility of these sensors. Among these criteria are:

a. sensitivity: 1-10 ppb,

b. time response: 10 sec,

c. reversibility: 30 sec,

d. shelf life: 6 months [estimated],

e. operational life: 10 days [estimated], and

f. compactness.

Sensitivity, time response, and reversibility are the more critical of these parameters.

Developed in the next report section ("General Theory of CHEMFETs") is the principle of operation of insulated-gate chemically sensitive field-effect transistors (IGFETs), and, thereafter (in "Types of CHEMFETs for Detection of

---

EDITOR'S NOTE: Also available is another publication on the subject of chemical warfare detectors--SAM-TR-80-21, A Coated Piezoelectric Crystal To Detect Chemical Warfare Agents In Aircraft, by G. G. Guibault, Y. Tomita, and E. S. Kolesar, Jr.

Chemical Warfare Agents"), the operation of the four CHEMFET types. At present, three of these types can be excluded a priori because they fail to meet one or more of the main criteria (sensitivity, time response, and reversibility). A brief review of these three types is included in this report, however, because a development in related sciences could possibly enable construction of such CHEMFETs. In that eventuality, this report could serve as a useful starting point.

Recommendations for further action are stated in the "Conclusions" section of this report.

GENERAL THEORY OF CHEMFETS

Of the several types of chemically sensitive semiconductor devices (CSSD) discussed in the literature, all depend in some way on the semiconductor field effect for their operation. The CHEMFET is no exception. Structurally, it is very similar to the IGFET, a device which is the basis for the integrated circuit revolution presently taking place in electronics. The theory of IGFETs is well developed, and is generally presented in the language of the electronics engineer or solid-state physicist rather than that of the chemist. The purpose of this report section is to outline those elements of the theory which are most useful to the reader in understanding and using ion-sensitive field-effect transistors (ISFETs). Hence, the metal-insulator-semiconductor (MIS) structure is briefly discussed here.

The Metal-Insulator-Semiconductor (MIS) Structure

The IGFET theory is based on the analysis of the MIS structure--a useful tool in the study of semiconductor surfaces. The MIS structure (Fig. 1), in its simplest form, consists of a "parallel plate capacitor" where the metal forms one plate and the semiconductor forms the other. The insulator, of thickness d, is assumed to be a "perfect" insulator; i.e., no charged species can be transported through it. This structure is considered to be a single system in a thermodynamic analysis. Equilibrium refers to the condition in which the free energy of the electrons in the metal and semiconductor are equal. The free energy of electrons in a solid is usually described in terms of the Fermi energy level, E_F. The same terminology is used in this discussion. Therefore, the MIS structure is in equilibrium when the Fermi level in the metal and that in the semiconductor are equal.

Ideal MIS Structure

The starting point for analysis of the MIS structure is the "ideal" MIS, which, by definition, has the following characteristics: (a) The electron work function of the metal, Φ_m, and that of the semiconductor, Φ_S, are equal (i.e., the metal-semiconductor work-function difference, Φ_{ms}, is zero). (b) The charge density in the insulator is everywhere zero. (c) No transport of any

---

EDITOR'S NOTE: Available, on p. 44, is a selective list (plus definitions) of the "Abbreviations, Acronyms, and Symbols" used throughout this report.

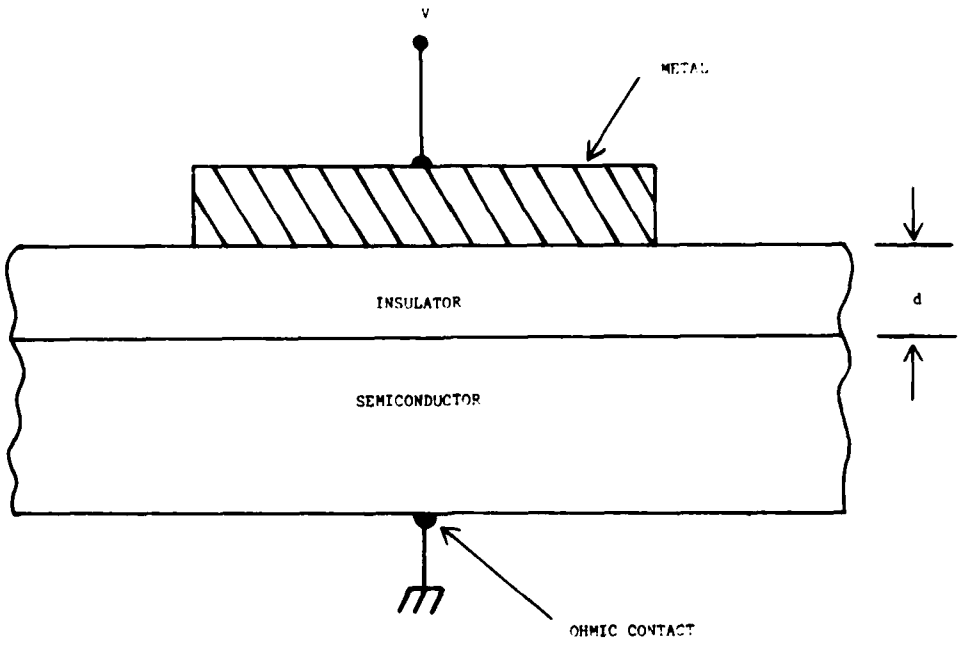

Figure 1. Typical metal-insulator-semiconductor structure used to study semiconductor electrical parameters.

charged species through the insulator takes place. (d) The ideal band structure of the bulk semiconductor extends to the surface (i.e., no surface states exist).

The analysis of the ideal MIS structure consists of calculating charge, electric field, and potential distributions throughout the structure as a function of an externally applied voltage difference between the metal and semiconductor. Thereafter, non-ideal effects which always occur in any real system can be considered and the three distributions (charge, field, and potential) can be recalculated. The non-ideal effects are: non-zero work-function difference; non-zero charge density in the insulator; interface charge layers; and deviations from the ideal semiconductor band structure at the surface (surface states).

The energy band diagram for the ideal MIS structure for a p-type semiconductor is shown in Figure 2.

The metal-semiconductor work-function difference, Φ_{ms}, is given by

$$\Phi_{ms} = \Phi_m - \left(\chi + \frac{E_g}{2} + \Phi_F\right) \qquad (1)$$

Note that χ is equivalent to the standard chemical potential of the electron, $\mu_{e,0}$.

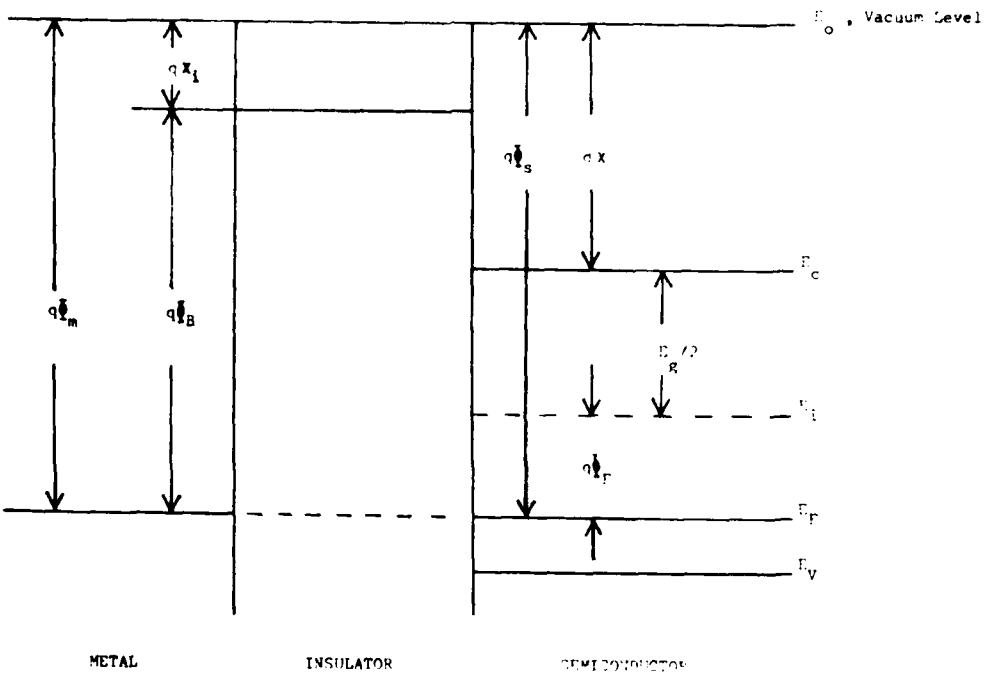

Figure 2. Metal-semiconductor energy-band level under flat-band conditions.

For the ideal MIS, $\Phi_{ms} \equiv 0$. The electron density, hole density, and net charge density in the semiconductor can be calculated in terms of the energy difference between the Fermi level, Φ_F, and any of the other defined levels, E_C, E_V, or E_i. The reader is referred to one of the standard texts on semiconductor physics for a detailed treatment (2, 37).

When a voltage, V_G, is applied between the metal and semiconductor, the "flat-band" condition of Figure 2 is changed. The Fermi levels in the metal and semiconductor become separated by the applied voltage. Since increasing electron energy upwards is customarily shown on the band diagrams, the application of a positive voltage to the metal relative to the semiconductor displaces the metal Fermi level downward relative to the semiconductor Fermi level.

Three states of charge distribution, depending on the sign and magnitude of the applied voltage, are in the semiconductor surface (Fig. 3). Under the "accumulation" condition, the negative voltage applied to the metal attracts additional holes to the semiconductor-insulator interface; i.e., holes accumulate at the interface. Because a very high density of holes is allowed near the top of the valence band, the accumulated layer of holes extends only a short distance into the semiconductor, and behaves much like a metal.

Under the "depletion" condition, the applied voltage, V_G, drives the mobile holes away from the surface--leaving behind a charge density composed of negatively charged acceptor atoms. For semiconductors used to fabricate IGFETs, this charge density is very much lower than the corresponding density of holes under accumulation. Therefore, the depletion space-charge region extends a considerable distance into the semiconductor. Electrostatic theory shows that the energy bands shift an appreciable amount within the space-charge region, as shown in Figure 3.

If a sufficiently large positive voltage is applied to the metal relative to the semiconductor, the bands will bend far enough to cause the intrinsic level, E_i, to cross the Fermi Level, E_F. In general, the hole density depends exponentially on the quantity $(E_i - E_F)$, and the electron density has a similar exponential dependence on the quantity $(E_F - E_i)$. Once E_i

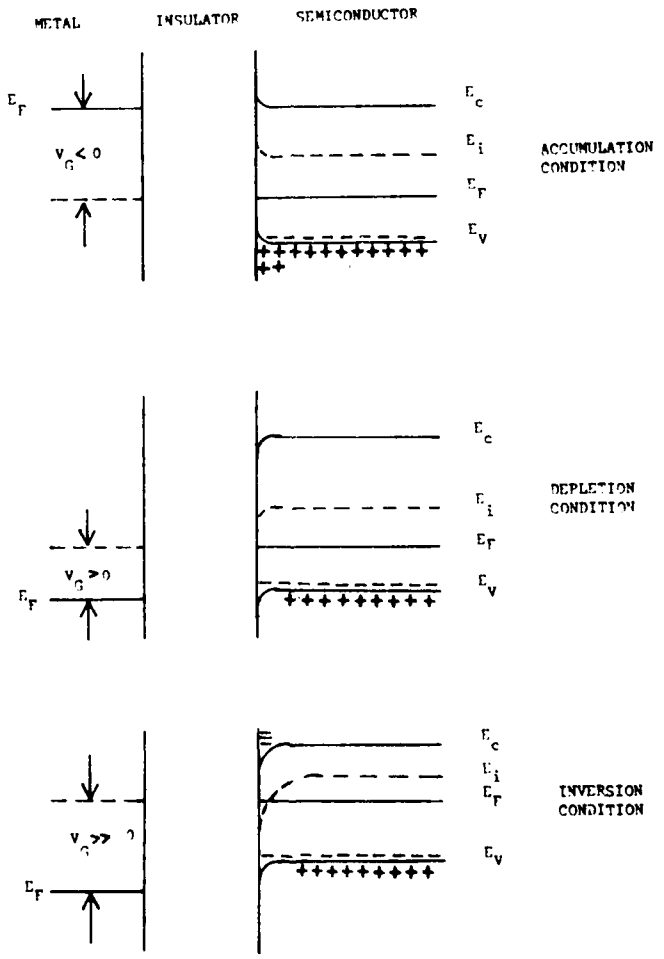

Figure 3. Metal-semiconductor energy level under bias conditions of interest. [+ = holes, mobile positive charges; - (above E_v) = negatively charged, immobile acceptor atoms; and - (above E_c) = mobile electrons in the conduction band.]

crosses E_F, the electron density exceeds the hole density, even though the dopant atoms normally make it p-type. Thus, the semiconductor is said to be in a surface "inversion" condition.

The band displacement corresponding to inversion can be seen (Fig. 2) to be $q\Phi_F$. For analysis of the IGFET, a more useful definition is that of "strong inversion." This condition occurs when the band displacement at the surface is $2\Phi_F$. The exponential dependence of electron density on $(E_i - E_F)$ means that the surface electron density increases very rapidly beyond the point of strong inversion. In other words, voltages applied to the metal (beyond that voltage required for strong inversion) increase the electron density in the surface inversion layer--but do not increase the band displacement at the surface. Applied voltage sufficient to bring about strong inversion is known as the threshold voltage, V_T; and, for the ideal MIS structure, is given by (ref. 2):

$$V_T = -\frac{Q_B}{C_o} + 2\Phi_F \tag{2}$$

in which Q_B is the charge per unit area within the surface space-charge region; and C_o is the capacitance per unit area of the insulator.

The number of mobile electrons per squared centimeter in the surface inversion layer becomes a linear function of $(V_G - V_T)$ for V_G greater than V_T. The principle of operation for the IGFET is the modulation of electrical conductivity in the surface channel by the applied voltage V_G.

The non-ideal effects that exist in a real MIS structure generally result in band-bending at the semiconductor surface, even with no externally applied voltage V_G. A non-zero work-function difference, $\Phi_{ms} \neq 0$, means that a charge flow must take place between the metal and semiconductor to bring about thermal equilibrium, thus resulting in a net charge separation in the system. The excess charge in the metal appears at the metal-insulator interface, while the excess semiconductor charge appears near the insulator-semiconductor interface. The band displacement in the semiconductor is the same as that which would result if a voltage equal to Φ_{ms} were applied to the ideal MIS structure. In Equation 2, V_T is the applied voltage necessary for strong surface inversion, starting from the flat-band condition of Figure 2. If $\Phi_{ms} \neq 0$, an applied voltage equal to Φ_{ms} must first be applied to bring about the flat-band condition; then an additional voltage, equal to that given in Equation 2, must be applied to bring about a strong surface inversion. In this case:

$$V_T = \Phi_{ms} - \frac{Q_B}{C_o} + 2\Phi_F \tag{3}$$

A non-zero charge density in the insulator can be analyzed in a similar manner. A charge in the insulator will induce an image charge in the metal and semiconductor. The induced charge in the surface of the semiconductor will result in band-bending at the surface, even for no externally applied

voltage. However, by application of the proper voltage, the image charge in the semiconductor can be cancelled to yield a flat-band condition (2). When Φ_{ms} and insulator charge distribution are considered:

$$V_T = \Phi_{ms} - \frac{1}{C_o} \int_0^d \frac{x}{d} \rho'(x)\, dx - \frac{Q_B}{C_o} + 2\Phi_F \qquad (4)$$

in which

d = insulator thickness,

x = distance measured from the metal insulator interface, and

$\rho'(x)$ = charge density in the insulator from all sources.

The most common MIS structure includes thermally grown SiO_2 on silicon. The charge distribution associated with this structure consists of a dense layer of positive charge, Q_{ss}, in the SiO_2 next to the silicon (effective at x = d). The usual practice in developing this theory defines a new insulator charge density $\rho(x)$ as:

$$\rho'(x) = \rho(x) + \delta(d)\, Q_{ss} \qquad (5)$$

in which $\delta(d)$ is the "delta" function.

Q_{ss} is the charge per unit area next to the Si/SiO_2 interface. Considering this non-zero charge density:

$$V_T = \Phi_{ms} - \frac{1}{C_o} \int_0^d \frac{x}{d} \rho(x)\, dx - \frac{Q_{ss}}{C_o} - \frac{Q_B}{C_o} + 2\Phi_F \qquad (6)$$

Another non-ideal effect which must be considered is the deviation from the ideal band structure in the form of a near continuous distribution of allowed energy levels across the "forbidden" band at the surface. These energy levels are known as "surface states." The influence of surface states on the voltage V_T is complex, and has been treated elsewhere (3). Fortunately, modern semiconductor technology can reduce the density of surface states to a negligible level, at least for thermally grown SiO_2 on silicon. The CHEMFET, which is the subject of this review, is fabricated with this SiO_2/Si system. Thus, surface states will not be seriously considered.

In the equation for V_T, the three terms which arise from the non-ideal properties of the real MIS are customarily grouped and are collectively

called: the flat-band voltage, V_{FB}. This is the voltage that must be applied to a real MIS structure to bring about the flat-band condition:

$$V_T = V_{FB} + 2\phi_F - \frac{Q_B}{C_o} \tag{7}$$

where

$$V_{FB} = \phi_{ms} - \frac{Q_{ss}}{C_o} - \frac{1}{C_o} \int_0^d \frac{x}{d} \rho(x)\, dx \tag{8}$$

The IGFET consists of a MIS structure with provisions for making electrical contacts to the surface inversion layer. The current-voltage relationship for this device is described in the following paragraphs.

Before proceeding further, some comment on the term "Field-Effect Transistor" may be instructive. The ability to deplete the density of mobile charge carriers and subsequently invert the surface is known as: the surface field effect. Equations 7 and 8, which describe this phenomenon, could have been derived in terms of electric fields at the surface instead of voltages across a MIS structure. In fact, the density of mobile charges in a surface inversion layer can be considered to be a measure of the electric field normal to the surface of the semiconductor. The surface field can be produced in two ways: The semiconductor can be built into a MIS capacitor and an external potential applied, as in the IGFET; or the field can arise from the electrochemical effects between different materials, as in the CHEMFET.

In either case, changes in the surface electric field change the density of mobile charge carriers in the surface inversion layer. The physical quantity measured is the change in electric current carried by the surface inversion layer; i.e., the drain current. Obviously, these devices must be operated under conditions that cause the surface inversion layer to form.

Current-Voltage Relationships for the Insulated-Gate Field-Effect Transistor (IGFET)

The typical construction and biasing arrangement for the n-channel IGFET are shown in Figure 4. In Figure 4, the semiconductor substrate (No. 3) forms one side of a parallel plate capacitor, and the metal gate field plate (No. 4) forms the other. In the normal operating mode, the gate voltage, V_G, is applied between the semiconductor substrate (No. 3) and the gate (No. 4). The polarity and the magnitude of V_G are selected so that the semiconductor field effect causes an inversion layer on the surface of the substrate under the gate. In fact, the surface of the p-type substrate (No. 3) becomes n-type. This n-type inversion layer forms a conducting channel between the source (No. 2) and drain (No. 1) regions. If this inversion layer is not present, application of a positive voltage, V_D, to the drain (No. 1) with respect to the source (No. 2) and substrate (No. 3) results in no appreciable

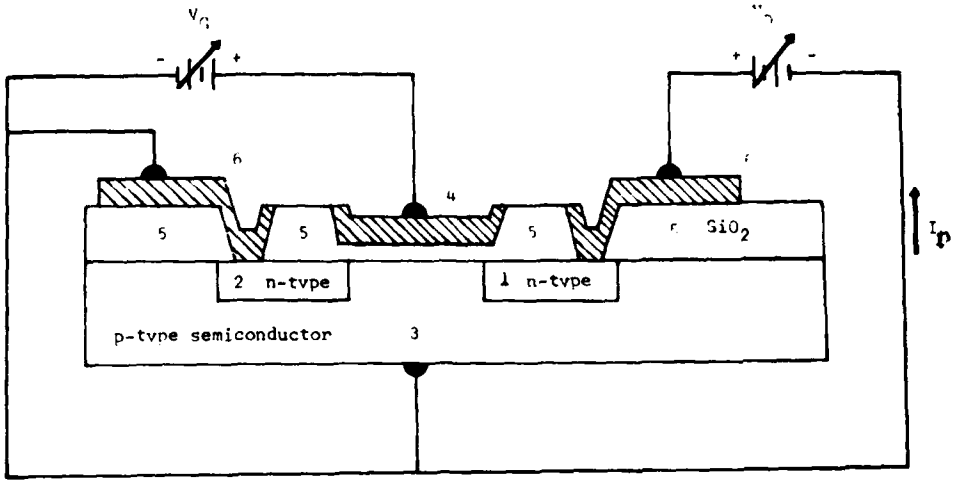

Figure 4. Cross-section of the n-channel metal-oxide-semiconductor field-effect transistor (MOSFET) structure. [1 = drain; 2 = source; 3 = p-type semiconductor substrate; 4 = metal gate; 5 = insulator; and 6 = metal contact.]

current flow, because the drain-to-substrate p-n junction diode is reverse biased. However, if an n-type inversion layer exists along the surface of the semiconductor between the source (No. 2) and drain (No. 1), a continuous path for the current, I_D, exists. As shown in Figure 4, the current, I_D, flows through the channel connection between the drain (No. 1) and source (No. 2). The magnitude of the drain current, I_D, will be determined by the electrical resistance of the surface inversion layer and the voltage difference, V_D, between the source and drain.

The basis for the derivation of the current-voltage relationship is the calculation of the density of the mobile electrons in the surface inversion layer, as a function of the applied voltages V_G and V_D, and of the position along the channel.

The IGFET channel region is depicted in Figure 5. At any point, y, along the channel, is found: a charge density, $Q_n(y)$, per unit area of mobile electrons in the surface inversion layer; and a charge density, $Q_B(y)$, of ionized dopant atoms in the space-charge region. These charge densities are a function of y because of the voltage change, along the channel, due to the drain current. Hence, Q_s, the sum of $Q_n(y)$ and $Q_B(y)$, is constant along the channel, and is equal and opposite to the charge per unit area of the metal plate which forms one side of the capacitor (the gate):

$$Q_s = Q_n(y) + Q_B(y) \tag{9}$$

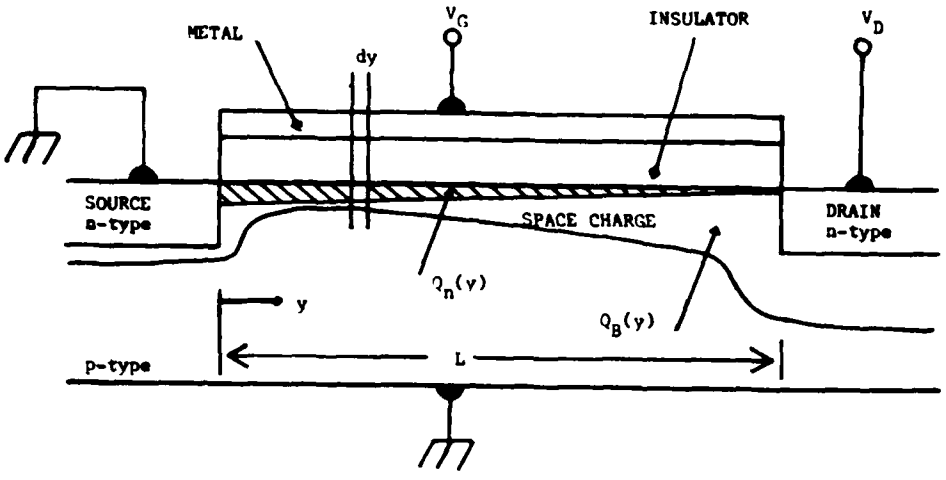

Figure 5. Cross-section of the field-effect transistor (FET) with small V_G.

Q_S may be related to the applied gate voltage and the capacitance C_o of the gate insulator by:

$$V_G - V_{FB} = -\frac{Q_s}{C_o} + \phi_s \tag{10}$$

where ϕ_S is the surface potential of the semiconductor.

The mobile electron charge in the surface inversion layer is given by:

$$Q_n(y) = -[V_G - V_{FB} - \phi_s(y)]\, C_o - Q_B(y) \tag{11}$$

In these equations, a surface inversion layer is assumed, in fact, to exist. At this point in the derivations, the assumption is made that the surface potential is given by the conditions of strong inversion:

$$\phi_s(y) = V(y) + 2\phi_F \tag{12}$$

Here, V(y) is the "reverse bias" applied to the "field-effect induced" p-n junction, composed of the n-type surface inversion layer and the p-type substrate.

$Q_B(y)$ is the charge in the space-charge region. By application of the "depletion approximation," the assumption is that no mobile charges are in the space-charge region:

$$Q_B(y) = - \sqrt{2K_s\varepsilon_o qN_A[V(y) + 2\phi_F]} \tag{13}$$

By collecting terms:

$$Q_n(y) = -[V_G - V_B - V(y) - 2\phi_F]\, C_o + (2K_2\varepsilon_o qN_A\,[V(y) + 2\phi_F])^{1/2} \tag{14}$$

By reference to Figure 5, the voltage drop along an element of channel, dy, can be written as:

$$dV = I_D dR = \frac{I_D\, dy}{W\mu_n\, Q_n(y)} \tag{15}$$

in which W is the width of the channel, and μ_n is the electron mobility in the channel.

Substituting Equation 14 for $Q_n(y)$ and integrating over the channel length yields the basic current-voltage relationship:

$$I_D = \frac{W}{L}\ \mu_n\, C_o \left\{[V_G - V_{FB} - 2\phi_F - \frac{V_D}{2}]\, V_D - \frac{2}{3}\sqrt{\frac{2K_s\varepsilon_o qN_A}{C_o}}\ [(V_D + 2\phi_F)^{3/2} - (2\phi_F)^{3/2}]\right\} \tag{16}$$

In the derivation of this equation, the surface inversion layer is assumed to exist at all points along the channel. From Equation 13, $Q_B(y)$ is seen to increase with V(y), the voltage drop along the channel. This increase is at the expense of $Q_n(y)$, the mobile channel charge. V(y) must change from 0 at the source to V_D at the drain; so, if V_D is large enough, the conducting channel will disappear at the drain. When this sequence occurs, Equation 16 is no longer valid and the IGFET is said to become "saturated."

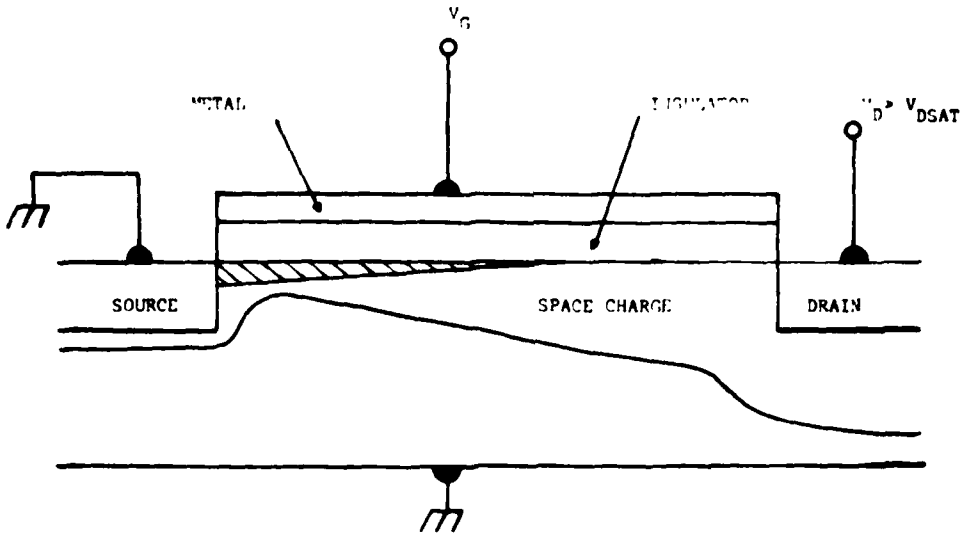

Figure 6. Cross-section of field-effect transistor channel region with saturated V_G applied. [V_{DSAT} = drain voltage at which surface channel narrows and disappears (near the drain).]

In the saturated IGFET (Fig. 6), V_{DSAT} is the drain voltage at which the surface channel narrows and disappears near the drain. An increase in V_D beyond V_{DSAT} results in the formation of a short space-charge region between the narrowest end of the surface channel and the drain. Current continues to flow, under these conditions, because electrons in the channel have no potential barrier to restrict flow from the end of the surface channel across the short space-charge region to the drain. However, the number of electrons arriving at the drain is determined by the voltage between the source and the end of the surface channel. This voltage, V_{DSAT}, can be shown to be (2):

$$V_{DSAT} = V_G - V_{FB} - 2\phi_F + \frac{K_s \varepsilon_o q N_A}{C_o^2} \left[1 - \left(1 + \frac{2C_o^2 (V_G - V_{FB})}{K_s \varepsilon_o q N_A} \right)^{1/2} \right] \quad (17)$$

For drain voltages greater than V_{DSAT}, the drain current, I_D, is given by Equation 16, with V_D replaced by V_{DSAT}, provided the surface channel length, L, is not appreciably shortened by the space-charge region existing between the end of the surface channel and the drain.

In Figure 7 the curves are divided, by the dashed line, into saturated and unsaturated regions. Note that V_{DSAT} is a function of the applied gate voltage.

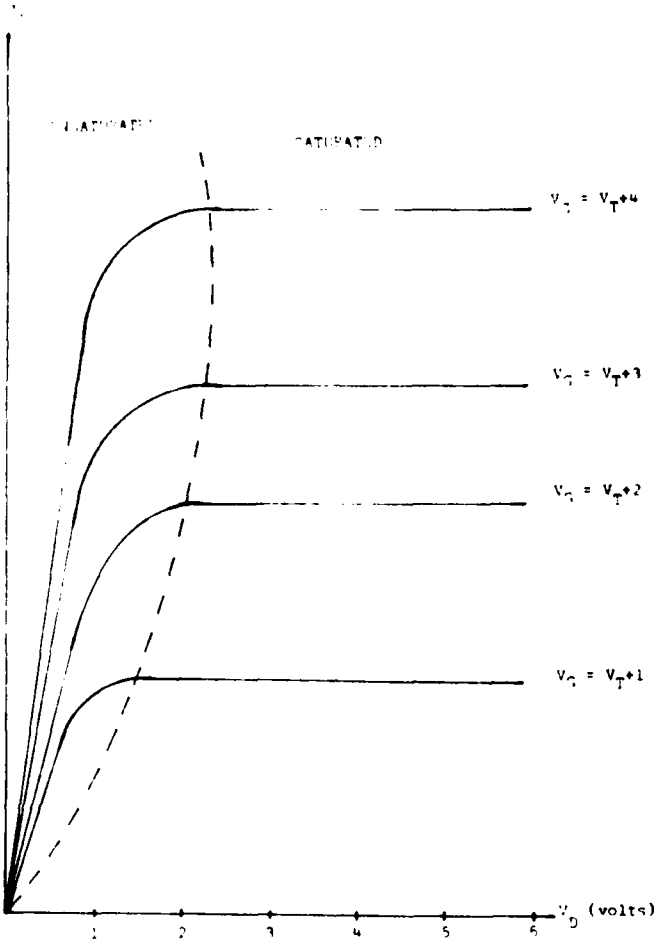

Figure 7. Family of I_D vs. V_D curves for a metal-oxide-semiconductor field-effect transistor.

Even though Equations 16 and 17 are derived via several simplifying assumptions, these equations are difficult to use because of their complexity. A much simpler set of equations may be derived if the dependence of $Q_B(y)$ [Eq. 13] on $V(y)$ is neglected. In this case:

$$Q_B = - \sqrt{2K_s\epsilon_o qN_A \, 2\phi_F} \tag{18}$$

and the integrations required to derive the current-voltage relationship can be simplified to yield:

$$I_D = \mu_n C_o \frac{W}{L} \{(V_G - V_T) V_D - \frac{V_D^2}{2}\}, \quad V_D < V_{DSAT} \tag{19}$$

where

$$V_T = V_{FB} + 2\phi_F - \frac{Q_B}{C_o} \tag{20}$$

and

$$V_{DSAT} = V_G - V_T$$

If no distributed charges are in the insulator or silicon surface states, the flat-band voltage, V_{FB}, reduces to:

$$V_{FB} = \phi_{ms} - \frac{Q_{ss}}{C_o}$$

Equation 19 is the current-voltage relationship for the unsaturated case. For drain voltages greater than V_{DSAT}, the current is given by Equation 19 with V_D being replaced by V_{DSAT}:

$$I_D = \mu_n C_o \frac{W}{L} \frac{(V_G - V_T)^2}{2} \qquad V_D > V_{DSAT} \tag{21}$$

Equations 19 and 21 are the IGFET current-voltage relationships most often quoted in the literature. Their use can lead to significant quantitative errors when currents are being calculated. They do, however, contain the

correct qualitative features of the device; i.e., the saturated and unsaturated regions, the near constant drain current beyond saturation, and the dependence of the saturation voltage on the gate and threshold voltages. Equations 19 and 21 have the distinct advantage of simple form.

Figure 8 is a plot of I_D vs. V_G for an n-channel "depletion mode" device. Depletion mode means that the device has a conducting channel for zero-applied gate voltage. Depletion mode n-channel devices are the result of a sufficiently negative flat-band voltage, V_{FB}. In the saturated regions--$V_D > (V_G - V_T)$; or, alternately, $V_G < (V_D + V_T)$--Equation 21 predicts a quadratic dependence of I_D on V_G. In the unsaturated region--$V_D < (V_G - V_T)$; or, alternately, $V_G > (V_D + V_T)$--Equation 19 predicts a linear dependence of I_D on V_G. Actual data, however, show a significant departure from linearity in the unsaturated region, as indicated in Figure 8. One contribution of this departure from theory is the variation of μ_n, the charger-carrier channel mobility with the electric field normal to the surface of the semiconductor. Surface channel mobility is primarily determined by surface scattering. Strong electric fields, that increase the probability of the carrier interacting with the surface, reduce the surface mobility. Therefore, as the gate voltage increases, the electric field normal to the surface increases and μ_n decreases.

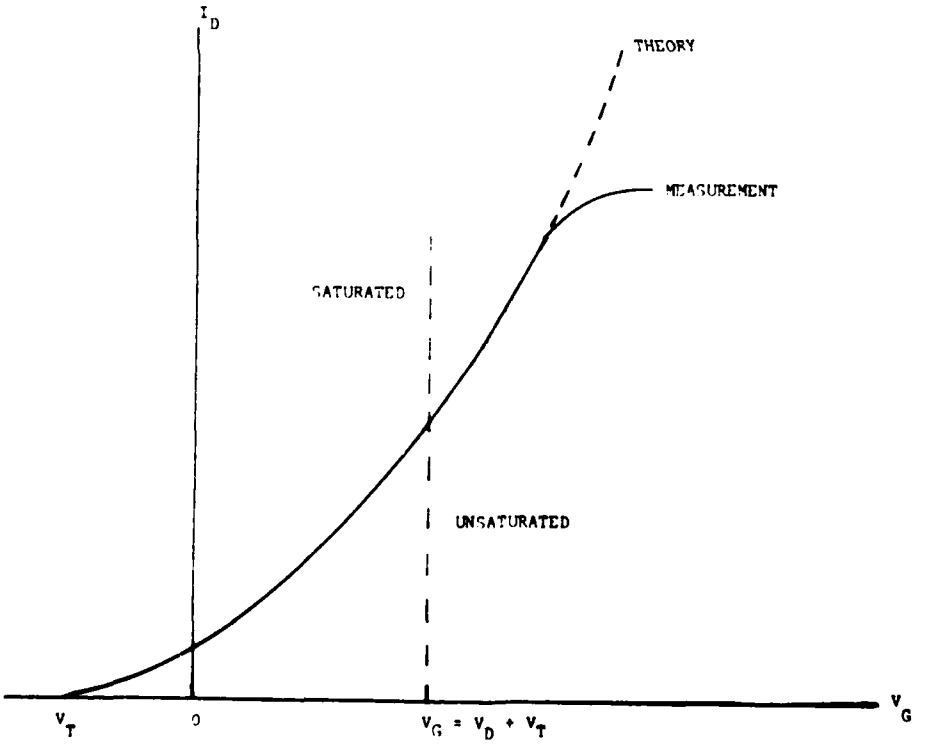

Figure 8. I_D vs. V_G curve for depletion mode device.

A second contribution to the departure of the I_D vs. V_G curve from linearity is series resistance between the end of the channel and the point at which the drain voltage is actually measured (Fig. 9).

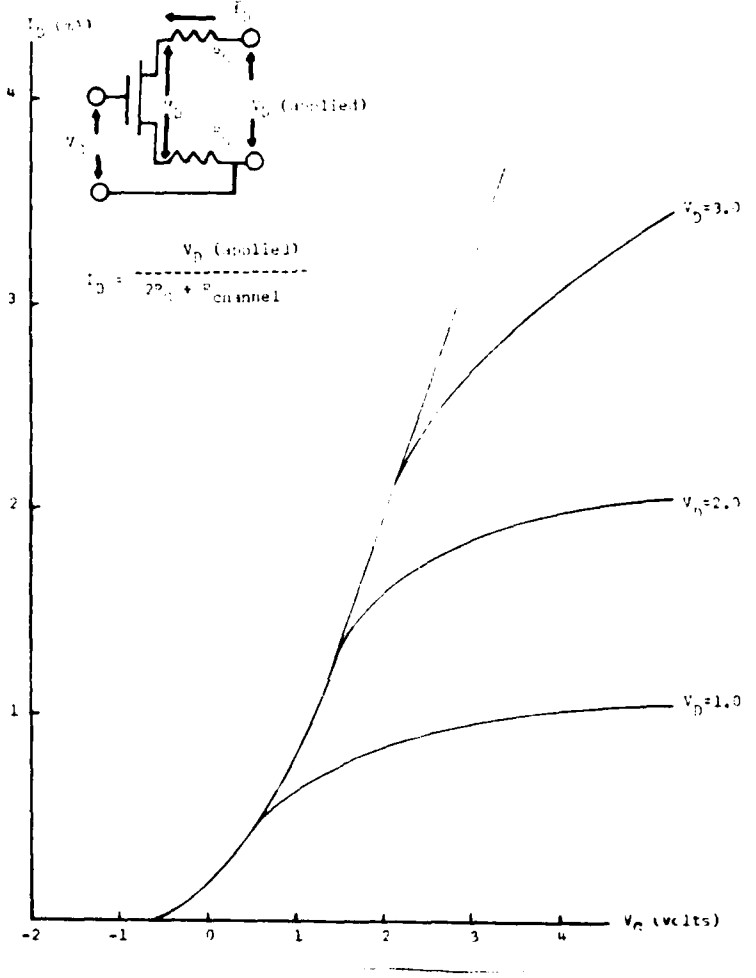

Figure 9. I_D vs. V_G curve deviation from ideality due to inherent resistance.

The resistive voltage drop reduces the effective drain voltage applied to the device. The magnitude of this resistance depends on individual device geometry and processing parameters. For example, in the case of the ISFET reported by Janata and Moss (4), the effective resistance for Figure 8 is 200 ohms. Their experimental data departs from linearity for drain currents of 2 millamperes (mA)--a value at which the 200-ohm resistance has an appreciable effect.

Because of the effects of non-ideal structures, second-order effects in parameters, and numerous approximations in the derivation of the current-voltage relationship, Equations 19 and 21 are used for a qualitative description of the actual device. Each individual design must be experimentally characterized.

For these reasons, and others, operating the CHEMFET in the constant drain current mode is advantageous.

Review of Assumptions

The derivation of Equations 19 and 21 applies the most common simplifying assumptions, the more important of which (a - e) are discussed here:

(a) One assumption is that a well-defined threshold voltage exists, and that formation of the surface inversion layer begins as the gate voltage is increased. This assumption is equivalent to stating that a sharply defined semiconductor surface potential divides surface depletion and surface inversion. In fact, this transition is continuous and, in conventional structures, is a good approximation when gate voltage exceeds "threshold voltage" by 0.5 volts.

(b) The voltage drop due to a surface channel current (drain current) has no effect on the thickness of the surface space-charge region. This approximation can yield large errors in the magnitude of predicted drain current in the saturation region, but the general shape of the drain current vs. drain voltage curves is satisfactory; i.e., the qualitative features of the device are not affected by this approximation.

(c) The doping of the semiconductor is constant near the surface where the channel is formed--not a good approximation for many ion-implanted structures.

(d) The channel length is large compared to the thickness of the depletion region surrounding the p-n junctions.

(e) The source and substrate of the device are connected to a common point in the external circuit.

Finally, under assumption (a), an equation relating the threshold voltage, V_T, to the device structure is given by Equation 20.

CHEMFET

In the case of the CHEMFET, the gate metal is replaced by: a complex structure consisting of a chemically sensitive layer (which may be part of the uppermost layer of the gate insulator); a solution containing the ions of interest; and a reference electrode. The terms in Equation 11, which are unique to the metal gate, must be replaced with quantities which describe the more complex CHEMFET structure.

According to the reaction characteristics of the species to be detected and to the chemically sensitive layer, CHEMFETs can be divided into three groups. These groups include devices, ISFETs, which will measure electrically neutral molecules. ISFETs are analogs of ion-sensitive electrodes (ISEs) and CHEMFETs, with a polarized solution-membrane interface.

CHEMFET Sensitive to Neutral Species

One CHEMFET structure sensitive to neutral species is the palladium (Pd) metal gate IGFET (5). Neutral hydrogen molecules under suitable conditions are reversibly absorbed by the palladium (6) which, in turn, affects the work function differential between the palladium and silicon and thus the flat-band voltage, V_{FB}, of the Pd-SiO_2-Si structure (Eq. 2). Also, Equation 8 indicates a corresponding change in the IGFET drain current, all other parameters remaining fixed.

Importantly, even though the hydrogen enters the Pd gate as a neutral species and changes V_{FB}, the Pd-gate H_2-sensitive IGFET must be operated with a charge return path so that the gate voltage can be defined in Equation 8.

The flat-band voltage, V_{FB}, is the sum of several terms. These terms include the metal-semiconductor work-function difference, the electrostatic effect of distributed charges in the insulator layer, and the interface states at the insulator-semiconductor boundary. The most developed IGFET structure, currently used for all CHEMFETs of practical significance, is the SiO_2-Si system. The microelectronics industry has achieved a detailed empirical understanding of this system.

Lundstrom and DiStefano (7) have suggested that "the change in energy barrier at the Pd-SiO_2 interface is attributed to an interfacial polarization layer and not to a change of the bulk metal Fermi level." In this case, this conclusion (7) does not apply because the flat-band voltage, V_{FB}, is not a function of this barrier energy. Rather, the charge equilibration in the IGFET system takes place via the charge return path, which consists of an electrical connection from the metal gate to the silicon. Charge equilibration does not take place by charge transport through the insulator; therefore, the barrier height for electrons between the Pd and SiO_2 cannot affect V_T.

If the absorbed hydrogen induces a charge separation across the SiO_2 layer, the situation is different. This situation would introduce a net charge on both the metal and semiconductor, and thus change the equilibrium charge distribution of the system. A simple electrostatic analysis (2) shows that the effect on V_{FB}, due to a net charge in the oxide, is proportional to the distance of the charge from the metal-oxide interface. If the charge in the oxide is very close to the metal, the change in V_{FB} is negligible. Thus, a dipole located at the metal-oxide interface has no effect on V_{FB}.

Another suggestion has been that neutral hydrogen atoms from the Pd-H_2 interaction enter the SiO_2, where they migrate to the SiO_2-Si interface and alter the interface state conditions--and this is the mechanism that results in the change of V_{FB} (8). However, this reasoning is contrary to the general experience of the silicon MOS (metal-oxide-semiconductor) integrated circuits industry. Hydrogen is widely used to "quench" the interface states in the Si-SiO_2 system. Proper annealing of the structure in hydrogen at elevated temperatures (above 400°C) will reduce to negligible levels the electrical effects of interface states.

The long-term stability (in years) of the devices at 150°C, or below, also attests to the stability of the hydrogen-quenched interface states. It

seems unlikely that hydrogen atoms generated by the H_2-Pd interactions would have greater mobility in SiO_2, and be less stable at the SiO_2-Si interface, than hydrogen atoms from the more conventional annealing steps. If hydrogen enters the oxide as a charged species with sufficient mobility to account for the rapid response of the hydrogen-sensitive IGFET, hydrogen would also drift rapidly under the applied gate voltage, thus making V_{FB} dependent on the magnitude of V_G. Hence the effect of hydrogen on the flat-band voltage is probably not due to charged hydrogen species in the oxide. The only acceptable mechanism that explains the device's behavior involves a change in the work-function difference between the palladium and silicon (5, 7-10). This effect can be achieved through a change either in the bulk chemical potential of the electrons in the palladium or, more likely, in the contact potential between the palladium and the contact metal.

The response of the Pd-gate FET to hydrogen is shown in Figure 10. The application of this sensor to smoke detection has been described by Lundstrom et al. (11). Another secondary response of the device is to gaseous hydrogen sulfide (12). Hydrogen sulfide (H_2S) readily dissociates at the palladium surface to sulfur and atomic hydrogen, which then diffuses into the palladium. The sensitivity of this device in air at 150°C is 1 mV (ΔV_T) per 2 ppm H_2S. The use of this type of device for detection of other dissociable molecules, such as NH_3, has also been suggested (13).

CHEMFET with Nonpolarized Interface--ISFET

Shown in Figure 11 is an ISFET structure in which the metal gate is replaced with a reference electrode, solution, and an ion-sensitive membrane. All other features of the device are protected by a suitable encapsulant. The heart of the ISFET is the gate. As shown in a preceding section ("Current-Voltage Relationships for the Insulated-Gate Field-Effect Transistor"), the gate voltage, V_G, controls the drain current, I_D, in Equations 9 and 21. To describe quantitatively the operation of the ISFET, a thermodynamic analysis of the structure is necessary (Fig. 12). This structure depicts the cross-section through the whole measuring circuit, including the reference electrode and the connecting leads. It is also the simplest case--one in which the reference electrode is of the first kind, described by the equilibrium equation:

$$M \rightleftharpoons M^+ + e^-$$

An example of this type of electrode is a silver wire immersed in a solution of silver ions. The solution is assumed to contain a small amount of ions which can permeate reversibly through the membrane, and a nonpolarized interface is formed.

An example would be a solution, containing 0.1 M $AgNO_3$ and 1×10^{-4} M KNO_3, in which the membrane would be potassium-ion sensitive. The insulator is assumed to be ideal; i.e., no charge can cross it, and it is thicker than

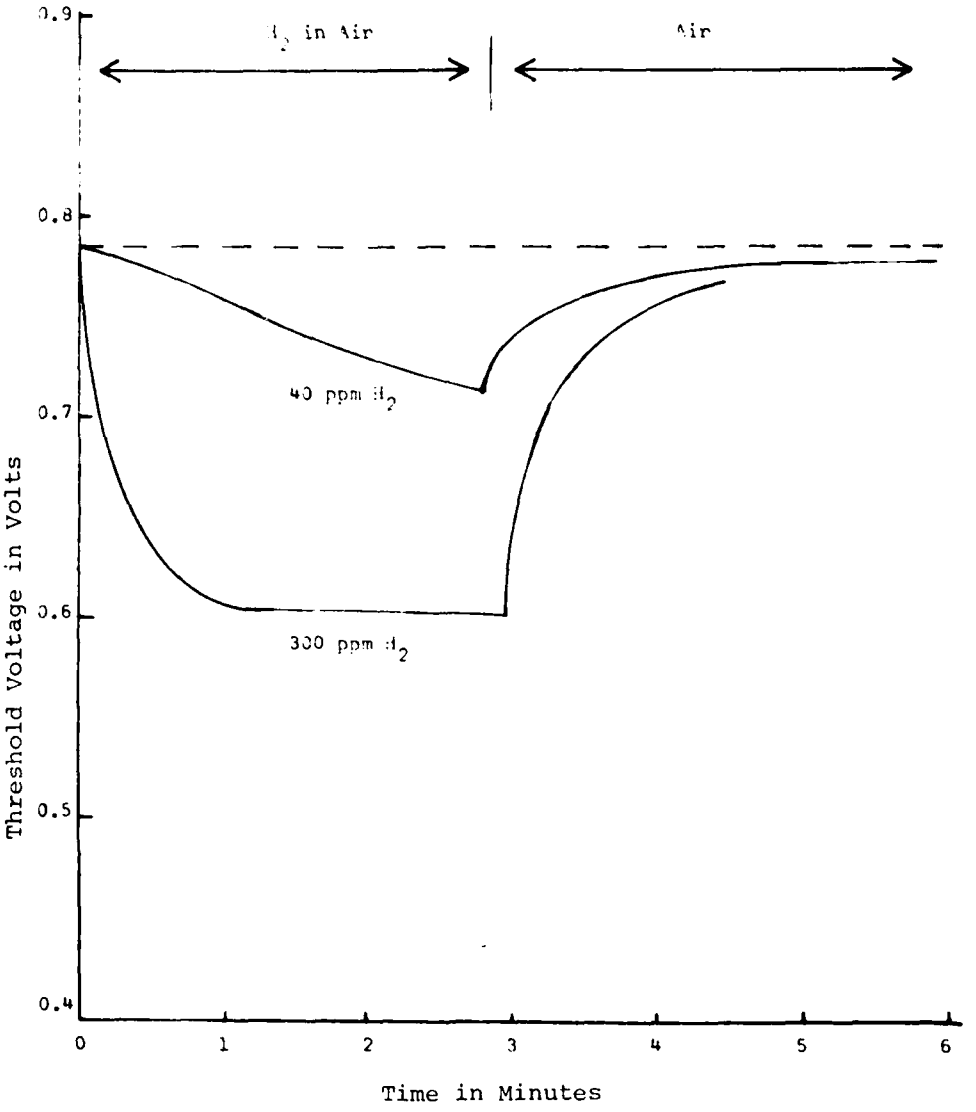

Figure 10. Response of palladium (Pd)-gate field-effect transistor to low levels of hydrogen.

the electron tunneling distance (d > 100 Å). [See "Authors' Note," below.] Layer 5 (Fig. 12) is the transistor semiconductor (such as silicon). The

---

AUTHORS' NOTE: In their recent paper, Bergveld et al. proposed a schematic diagram representing all CSSDs, including ISFETs (Fig. 2, in Ref 8). In their structure, the measured species are shown to move within the whole structure of the device. We suggest that, if these species carry an electric charge, Bergveld's structure cannot represent a CHEMFET in any form--because charge can neither move within the gate insulator nor cross boundaries with the adjacent layers. This point has its implications on the equilibrium condition of the CHEMFET (vida infra).

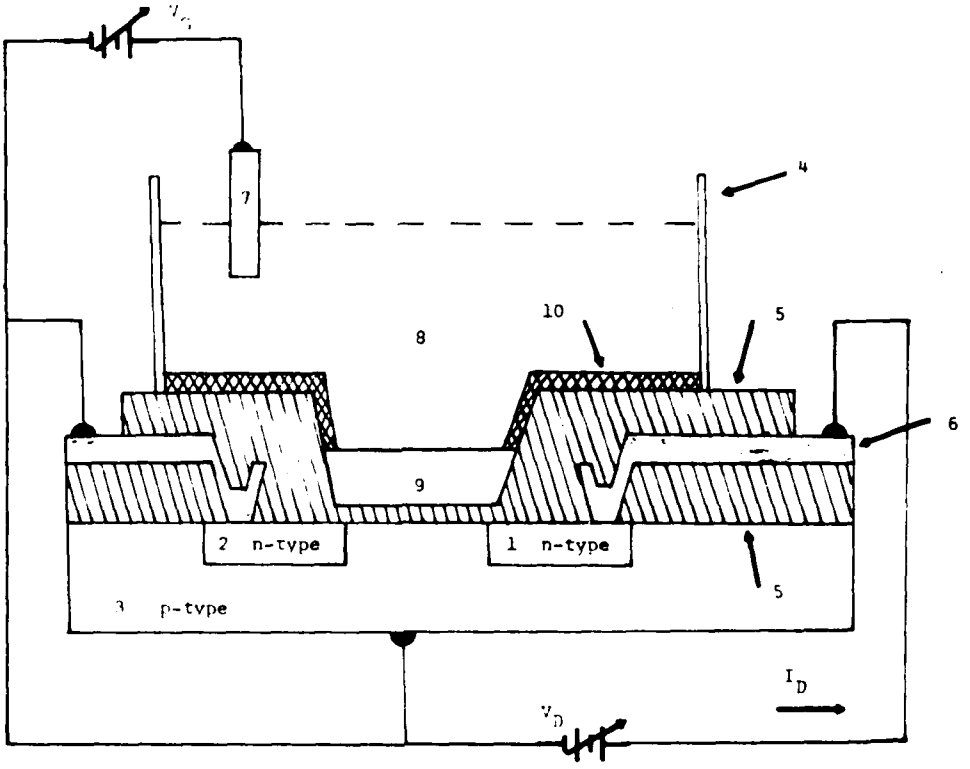

Figure 11. Ion-sensitive field-effect transistor in solution. [1 and 2 = n-type semiconductors; 3 = p-type silicon; 4 = solution retainer; 5 = insulator; 6 = metal contact; 7 = reference electrode; 8 = solution; 9 = ion-sensitive membrane; and 10 = suitable encapsulant.]

metal (Fig. 12: No. 6) will be identical to that in the reference electrode (No. 1). The switch, SW, represents operation of the device when it is closed.

The charge, field, and potential profiles across the structure are shown in Figure 12. This is, of course, a very simplified case. Omitted, for the sake of simplicity, are: liquid junction; dual layer insulator; trapped charges in the insulator; surface states at the insulator-semiconductor interface; channel doping; and a multitude of connecting metals. Similar charge, field, and potential profiles accounting for some of these elements have been published (4, 14-16).

From a thermodynamics point of view, this is a multiphase system where the Gibbs equation applies at equilibrium:

$$\Sigma_i \, dn_i \, \mu_i = 0 \qquad (22)$$

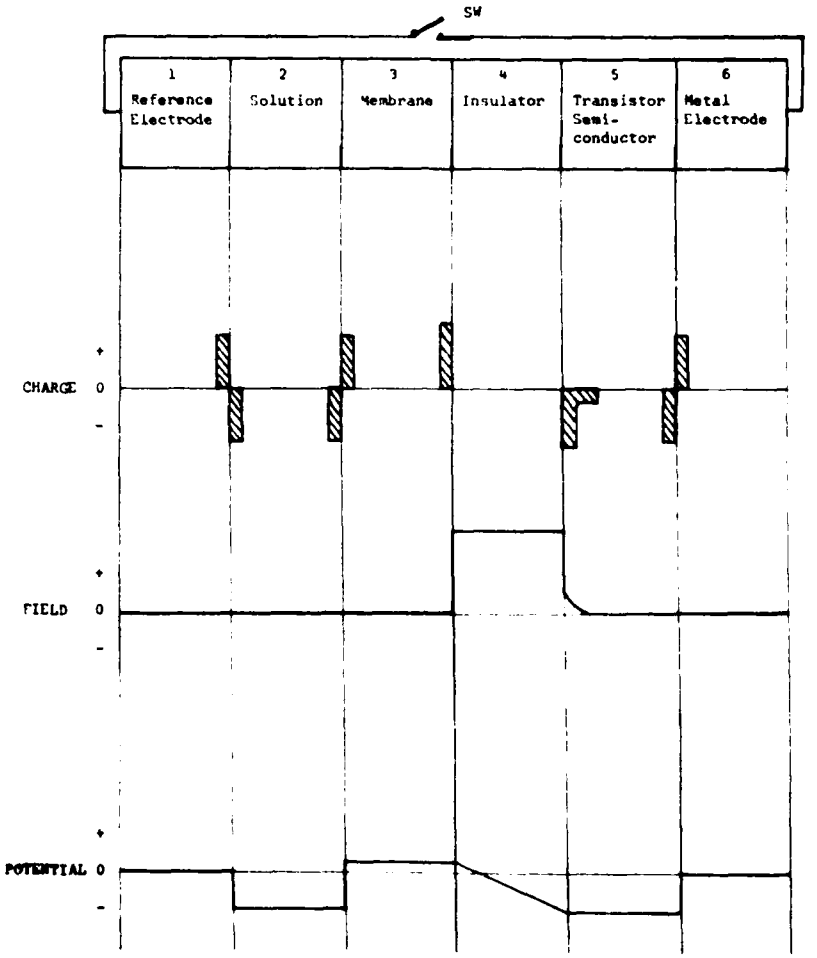

Figure 12. Cross-section of the ISFET structure shown in Figure 11, as well as the local charge density, electric field, and variations in potential.

in which dn_i is the number of moles of "species i" transported across individual interfaces, and μ_i is the electrochemical potential of species i. Equation 22 can be expanded to yield the relationship:

$$\tilde{\mu}_3 \equiv \tilde{\mu}_2 \equiv \tilde{\mu}_1 \equiv \tilde{\mu}_6 \equiv \tilde{\mu}_5 \qquad (23)$$

which simply expresses the fact that, in the case of an ideal insulator (Fig. 12: No. 4), the only way this system can reach equilibrium is through the external pathway (Nos. 1 and 6). If the switch, SW, is open, the

situation is equivalent to operation without a reference electrode (or a signal return). Thus:

$$\tilde{\mu}_1 \neq \tilde{\mu}_6 \tag{24}$$

The inequality of Fermi levels in metals (Fig. 12: Nos. 1 and 6) results in the inequality of $\tilde{\mu}_3$ and $\tilde{\mu}_5$. Thus, the basic condition for stable operation of the ISFET is not satisfied.

As mentioned in the "Introduction," some researchers originally claimed that ISFETs could be operated without a reference electrode as a single-ended probe (17-21). This point of view has been contested (4, 14-15, 22), and it is now agreed that a signal return (reference electrode) is necessary for stable direct-current operation. Controversy still exists, however, as to whether ISFETs sensitive to electrically neutral species can or cannot be operated without a reference electrode (as already discussed in the section on "CHEMFET").

Following is an analysis of the circuit in Figure 12. The inner potential in the semiconductor (No. 5) can be expressed as:

$$\phi_5 = \frac{1}{F} \left(\mu_5^e - \tilde{\mu}_5^e\right) \tag{25}$$

in which μ_5^e is the chemical potential of an electron in the semiconductor (the electron-lattice interaction energy), and $\tilde{\mu}_5^e$ is the electrochemical potential of an electron in phase 5, commonly known as the Fermi level. Similarly, for the membrane (Fig. 12: No. 3) the inner potential, ϕ_3, is:

$$\phi_3 = \frac{1}{z^i F} \left(\tilde{\mu}_3^i - \mu_3^i\right) \tag{26}$$

in which z^i, the number of elementary charges, is positive for cations and negative for anions; and $\tilde{\mu}_3^i$ and μ_3^i are the respective electrochemical and chemical potentials of species i in phase 3. The potential difference across the insulator and semiconductor space-charge region is:

$$\phi_5 - \phi_3 = \frac{1}{F} \left(\mu_5^e - \tilde{\mu}_5^e\right) - \frac{1}{z^i F} \left(\tilde{\mu}_3^i - \mu_3^i\right) \tag{27}$$

It is now essential to identify the relationship between species i in the membrane (No. 3) and an electron in the semiconductor (No. 5).

We know that ion i can transfer from the solution (Fig. 12: No. 2) into the membrane (No. 3). Thus, according to Equation 23, the electrochemical potentials of ion i in the two phases must be equal:

$$\tilde{\mu}_3^i = \tilde{\mu}_2^i = \mu_2^i + Z^i F \phi_2 \tag{28}$$

where ϕ_2 is the inner potential of the solution. Similarly, Fermi levels in the semiconductor and the metal (Fig. 12: No. 6) are equal. Because the metal (No. 6) was defined to be the same as the metal (No. 1: the reference electrode), then:

$$\tilde{\mu}_5^e = \tilde{\mu}_1^e = \mu_1^e - F\phi_1 \tag{29}$$

An equilibrium also exists in the metal between the cations and electrons:

$$M_1 \rightleftarrows M_1^+ + e_1^-$$

for which we can formally write:

$$\mu_1^M = \mu_1^{M^+} + \mu_1^e \tag{30}$$

Substituting for μ_1^e in Equation 29 yields:

$$\tilde{\mu}_5^e = \mu_1^M - \mu_1^{M^+} - F\phi_1 \tag{31}$$

Combining and rearranging Equations 27, 29, and 31 yields:

$$\phi_3 - \mu_3 = \frac{1}{F}(\mu_5^e - \mu_1^M + \mu_1^{M^+}) - \frac{1}{z^i F}(\mu_2^i - \mu_3^i) + (\phi_1 - \phi_2) \qquad (32)$$

The first term on the right-hand side of Equation 32 represents the contact potential between semiconductor and metal. Also:

$$\phi_5 - \phi_1 = \frac{1}{F}(\mu_5^e - \mu_1^e) = \Delta\phi_{cont} \qquad (33)$$

The second term can be related to the solution activity of the ion (Nernst equation):

$$\frac{1}{z^i F}(\mu_2^i - \mu_3^i) = E_o^i + \frac{RT}{z^i F} \ln a_2^i \qquad (34)$$

where a_3^i is assumed to be constant and is included in term E_o^i. Finally, $(\phi_1 - \phi_2)$ is the reference electrode potential, E_{REF}. Equation 32 can now be written as:

$$\Delta\phi_{3/5} = \phi_3 - \phi_5 = \Delta\phi_{cont} + E_o^i + \frac{RT}{z^i F} \ln a_2^i - E_{REF} \qquad (35)$$

This equation is essentially identical with that derived by Buck and Hackleman (15). The voltage across the gate insulator $\Delta\phi_{3/5}$ can be superimposed on an externally applied voltage, V_G, which has the same meaning and function as defined in the theory of operation of the IGFET (in the section on the "Current Voltage Relationships for the Insulated-Gate Field-Effect Transistors").

Combining Equations 19 and 35 yields:

$$I_{DS} = \frac{\mu_n C_o W V_D}{L}\left(V_G + \Delta\phi_{cont} + E_o^i + \frac{RT}{z^i F} \ln a_2^i - E_{REF} + \frac{Q_{ss}}{C_o} - 2\phi_F + \frac{Q_B}{C_o} - \frac{V_D}{2}\right) \qquad (36)$$

Defining V_T^* for the ISFET yields:

$$V_T^* = -\Delta\Phi_{cont} - E_o^i - \frac{Q_{ss}}{C_o} + 2\phi_F - \frac{Q_B}{C_o} \qquad (37)$$

The inclusion of the term E_o^i (but not E_{REF}) in the threshold voltage is arbitrary. The reason is that the membrane is physically part of the ISFET, and thus its standard potential should be included in V_T^*. On the other hand, the reference electrode is a completely separate structure. The final equation, for the drain current of the ISFET sensitive to the activity of ions i, is:

$$I_D = \frac{\mu_n C_o W V_D}{L} \left(V_G - V_T^* \pm \frac{RT}{z^i F} \ln a_2^i - E_{REF} - \frac{V_D}{2}\right) \qquad (38)$$

for operation in the unsaturated region; and

$$I_D = \frac{\mu_n C_o W}{2L} \left(V_G - V_T^* \pm \frac{RT}{z^i F} \ln a_2^i - E_{REV}\right)^2 \qquad (39)$$

for operation in the saturated region.

In the previously derived drain-current equations, the reference electrode potential was missing (19); and the poorly defined "membrane-semiconductor" (4, 23), or "liquid-semiconductor" (24) work-function difference, was used instead of the contact potential.

An opinion exists that the thermodynamics of ISFETs is undefined because the "reversible potential cannot be defined at the membrane-insulator interface." Electroanalytical chemists often refer to nonpolarized electrodes as "reversible." A polarized electrode is also thermodynamically reversible; but it has one more variable (usually, charge) than a nonpolarized electrode--that is, the interfacial potential can be measured directly only if the charge density can be kept constant. Otherwise, the potential is observed to "drift." This point has already been discussed in greater detail elsewhere (16). "Nonreversible membrane-insulator interface" means a polarized interface; i.e., a charged species cannot cross it. This reasoning is indeed true, because the insulator is considered to be ideal; and, for the voltages involved in these measurements, it behaves like an ideal insulator. In summary, a nonpolarized interface is unnecessary because the charge transport stops at this interface.

TYPES OF CHEMFETS FOR DETECTION OF CHEMICAL WARFARE AGENTS

Enzyme-Coupled CHEMFET

The enzyme-coupled CHEMFET is a direct analog of the cholinesterase electrode investigated by other groups (25-29). Its principle of operation is shown in Figure 13. The underlying transistor structure is the same as that of the ISFET already discussed (in the section on the "General Theory of Chemically Sensitive Field-Effect Transistors"). The enzyme-containing layer (Fig. 13: No. 1) is placed on top of the acetylcholine (or choline) sensitive membrane (No. 2); and the substrate is dissolved in solution (No. 3). The change of potential is related to the enzyme activity (28) which, in turn, is controlled by the presence of inhibitors such as chemical warfare (CW) agents.

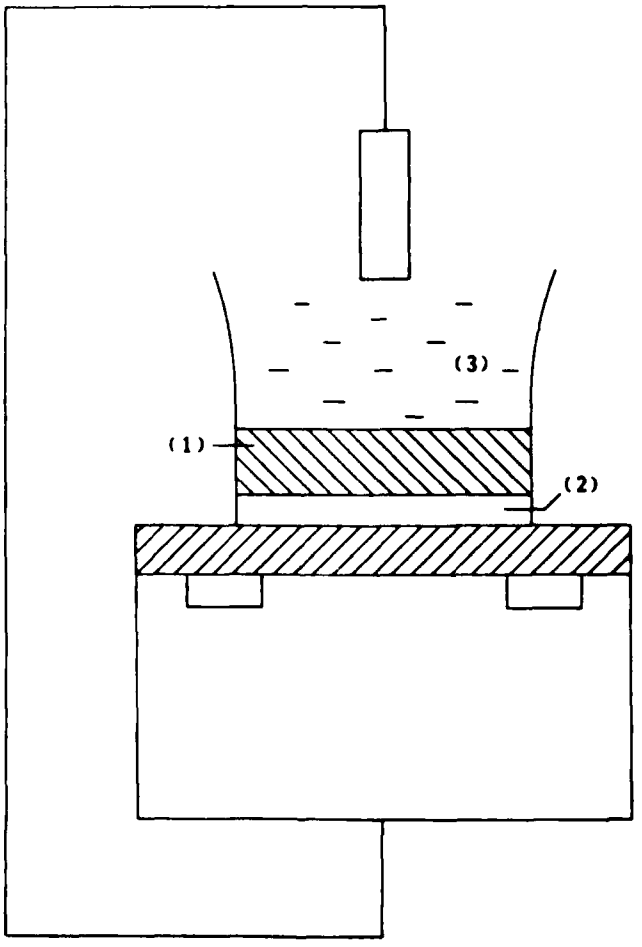

Figure 13. Structure of enzyme-sensitive field-effect transistor. [(1) enzyme-containing layer; (2) choline-sensitive membrane; and (3) solution.]

The most significant advantage of such a system is its high sensitivity which is due to the high turnover rate of the enzyme. The small size of the active area of the CHEMFET (1,000 - 10,000 μ^2) would reduce the amount of enzyme needed, thus reducing the cost.

Feasibility of the Enzyme-Coupled CHEMFET

The main disadvantage of this type of CW detector is its irreversibility. Also, the continous consumption and/or hydrolysis of the substrate limits the usable lifetime to hours rather than days (27, 28).

Our conclusion is that this type of CHEMFET fails to meet the condition of reversibility and lifetime. Possibly, the consumption of the substrate could be reduced while the device is "on the shelf"--or the effect of spontaneous hydrolysis could be minimized (27). However, the very nature of the action of CW agents (i.e., irreversible inhibition of cholinesterase) makes rather dubious the prospect of this type of detector.

Galvanostatic CHEMFET

An oxygen-sensitive FET has been postulated (30) which would operate on galvanostatic principles. In this device (Fig. 14), the electrochemical cell consists of a working electrode (No. 1), a counter electrode (No. 2), and a solid-state electrolyte (No. 3) that are placed on top of the insulator of a conventional MOSFET. The gas to be analyzed diffuses into the electrolyte (No. 3), and is reduced or oxidized on the working electrode (No. 1). The voltage which develops between the two electrodes depends on the electrochemical reactions. The feasibility of this approach depends on whether the respective species undergoes an electrochemical reaction or has an inhibiting or enhancing effect on another electrode reaction. Since the absolute detection limit for a direct oxidation-reduction is approximately 10^{-5} M (in aqueous solutions), obtaining sufficient sensitivity would be unlikely even if the direct reduction or oxidation of a CW agent were possible.

The catalytic effect (i.e., enhancement of the electroreduction-oxidation of another substrate) offers some potential. Assume that the hypothetical reduction of substrate oxidation takes place in the electrochemical cell shown in Figure 14.

The current-voltage relationship is shown in Figure 15, curve a, where the concentration of oxidation is assumed to be high ($> 10^{-2}$ M). If the overvoltage required for this process can be lowered by the presence of a CW agent, the current-voltage relationship can be represented by curve b. The two dashed horizontal lines represent a superimposed constant current. The intercepts of these lines with current-voltage (I-V) curves in the absence (a) or presence (b) of a CW agent represent the voltage (E_a or E_b, respectively) across the electrochemical cell. If the working electrode is placed at the top of the solid-state electrolyte and the counter electrode is connected, as shown in Figure 14, then the change in the polarizing voltage will be manifested by the change of the drain current.

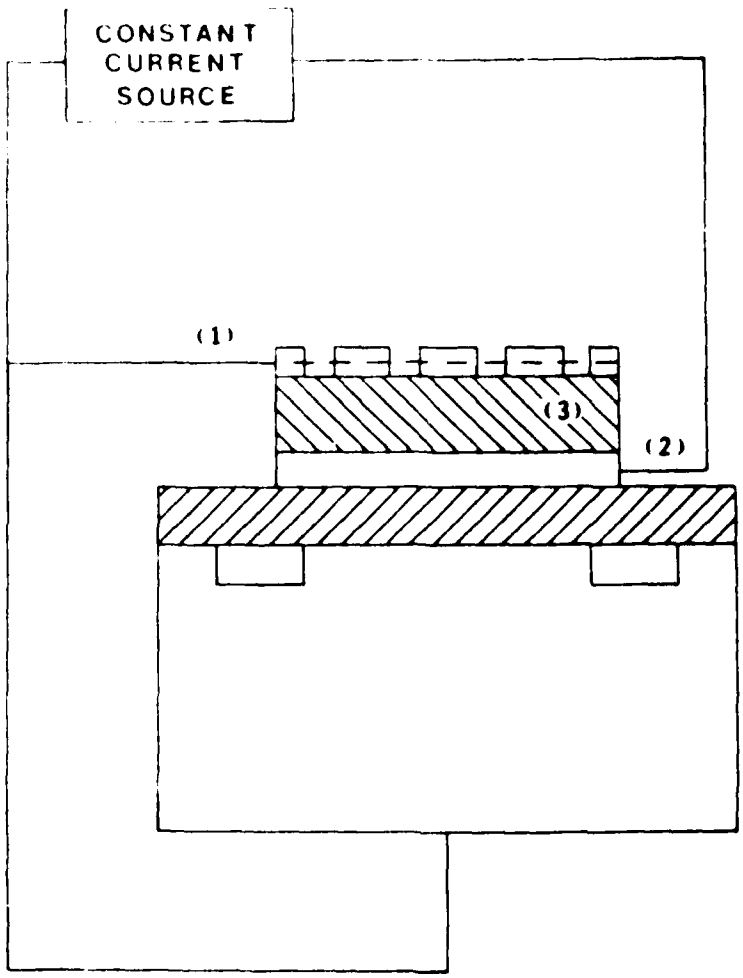

Figure 14. Structure of galvanostatic type of field-effect transistor. [(1) working electrode; (2) counter electrode; and (3) solid-state electrolyte.]

In Figure 15, the vertical lines show a voltage limit (i.e., zener diode in parallel with the cell) which can be applied at the electrodes. Thus, the electroreduction of the substrate oxidation would never take place in the absence of CW agent. This feature would lend itself to coupling a suitable alarm mechanism to the device. The same argument can be applied to a system in which a CW agent catalyzes the oxidation of a substrate.

Feasibility of the Galvanostatic CHEMFET

This system is, essentially, an electrochemical cell coupled with an integrated circuit. Many unknowns are involved in this scheme. (The electrochemistry of CW agents in solid-state electrochemical cells is not known by

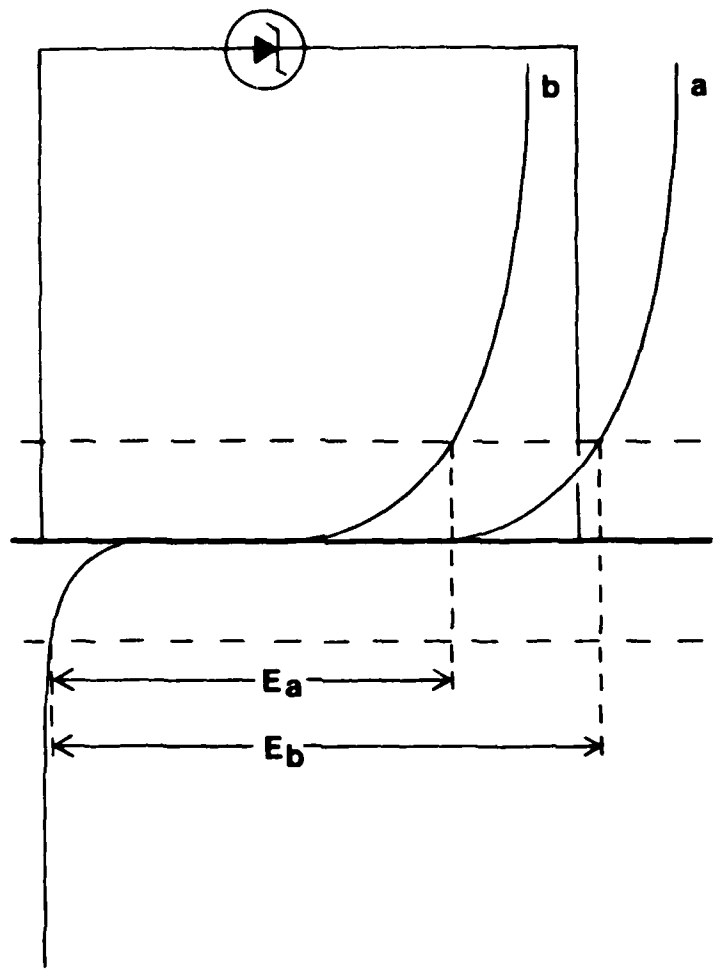

Figure 15. Current-voltage (I-V) curve of the hypothetical electrochemical cell. [Curve a = concentration of oxidation is high; Curve b = overvoltage lowered by CW agent; E_a = voltage with CW agent absent; and E_b = voltage with CW agent present.]

the authors.) The solid electrolyte galvanic cells for gas sensing usually suffer from slow time response (31). This problem could be mitigated by ensuring that the working electrode is at the top of the device, thus minimizing the diffusion distance. This concept offers some possibility, particularly because conventional catalytic currents permit detection of species down to 10^{-8} M concentrations. However, a thorough knowledge of the electrochemistry of CW agents in solid-state electrolytes, particularly their electrocatalytic properties, is a prerequisite.

Catalytic CHEMFET

The principle of operation of the catalytic CHEMFET is shown in Figure 16. A layer of CW agent reactive polymer (No. 1) is placed on top of the ISFET (No. 2). The catalyzed decomposition of the CW agent takes place inside the membrane. Products of the composition reaction (No. 1) diffuse towards the ISFET membrane, where they cause a potential difference. Note that a "solid" contact (No. 3) to the catalytic layer could be formed with a gel reference electrode.

Feasibility of the Catalytic CHEMFET

a) With a catalytic CHEMFET, the diffusion of products through the catalytic membrane and substrate limits the time response--typically on the order of minutes (32). The device would thus fail on the basis of time response.

b) The sensitivity of ion-selective membranes is typically 10^{-6} M. Membranes with higher sensitivity (10^{-17} for S^{--}) have been reported, however; and these must be operated under special conditions (i.e., special ion buffers). It should be noted that a hydrogen ion cannot be used as the indicator ion, because the concentration range of CW agent is below the dissociation constant of water (10^{-7} at 25°C). Fluoride is one of the possible products which could be detected using an F^- ISFET. However, the sensitivity of LaF_3 membranes is 10^{-6} M F^-, at best. Therefore this sensor would fail with respect to sensitivity.

Work-Function Dependent CHEMFET

To build a work-function dependent, gas-sensitive CHEMFET requires a gate material whose work function can vary several orders of magnitude in the presence of small concentrations of a CW agent. Any material whose work function (or Fermi Level) is a sensitive function of composition will probably be a semiconductor. In general, metals are inappropriate because they have a high density of electrons and large amounts of gas absorption would be required to change their electrical properties. Insulators would be useless, since the gate material must make an electrical connection to the circuit. To interact specifically with a particular CW agent, the prospective gate material must possess special chemical properties and probably will have to be an organic material. Recent research in polymer chemistry has yielded several semiconducting polymer materials (33). Many of these materials can have their electrical properties changed by many orders of magnitude through a process analogous to the doping of inorganic semiconductors. This doping is accomplished by hanging side chains on the backbone of the polymer chain; if these side chains can couple into the electrically conducting bands of the main chain, they may donate or accept electrons in a manner similar to that of the single atom impurity donors or acceptors used in inorganic semiconductors to create n- or p-type semiconducting devices (33). Thus, if it is possible to place, in this way, side chains containing an organic complex that reacts readily with one particular gaseous agent to produce electrons (or electron acceptors) which interact with the main chain of an appropriate semiconducting polymer, one can produce a CHEMFET device which will sense that particular gaseous agent.

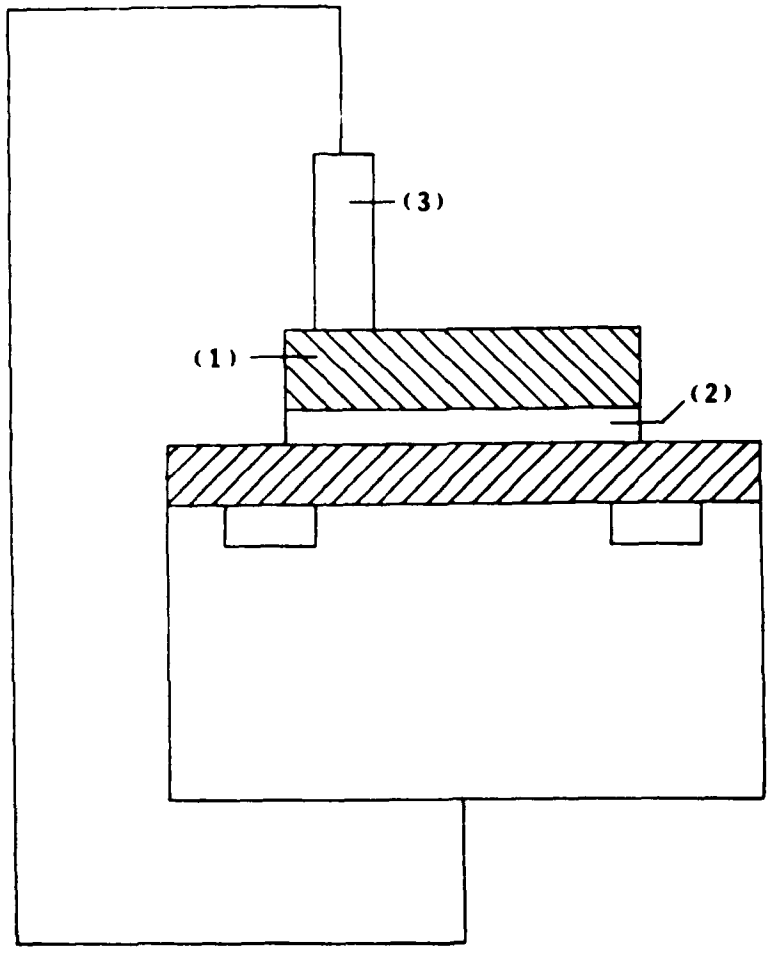

Figure 16. Structure of the catalytic-based field-effect transistor. [(1) a layer of CW agent reactive polymer; (2) the ISFET membrane; and (3) a "solid" contact to the catalytic layer.]

Although such a specifically reacting, semiconducting material might be made through today's technology, a number of unanswerable, or partially answerable, questions arise. These questions include reversibility, response time, resistance to poisoning, ability to form an electrical contact, and sensitivity.

For a device to be reversible, the polymer must maintain chemical equilibrium with the species in the gaseous phase, and must not make a permanent or near-permanent bond with the gaseous agent. On the other hand, to make a sensitive device, one must be able to fabricate a polymer with a high affinity for the particular agent.

It is desirable to build a detector with a short time response. To do so requires a polymer structure that is relatively loose, to reduce the diffusion coefficient, and that is as thin as possible. The first condition requires proper application of polymer chemistry to minimize diffusion time. The

second condition can be met with micron- or submicron-thin films. Submicron films are technically feasible; however, if the film's thickness approaches the Debye length of the conducting species (electrons or holes), the device sensitivity will be reduced. Since the device sensitivity is increased (as shown in the following) by using a polymer with a low initial concentration of conducting species (and, therefore, larger Debye length), one must be aware of this potential trade-off between response time and sensitivity.

Calculations of the Debye length and diffusion length provide estimates of the acceptable film thickness and the CW agent diffusion coefficient needed to satisfy the detection system specifications.

The Debye length describes the screening of electrostatic potentials by the rearrangement of mobile charge carriers, and varies inversely as the square root of the charge carrier concentration. A Debye length of 1 μm (10^{-4} cm) or less requires a carrier concentration of approximately 1 x 10^{13} or higher.

In order to meet the response time requirement of a few seconds, the CW agent species must diffuse through the membrane in a few seconds. To achieve a diffusion length of 10 μm in 10 sec will require a diffusion coefficient greater than 2.5 x 10^{-8} cm^2/sec.

For a CHEMFET device to work, the gate (as well as the rest of the device) must be in a well-defined thermodynamic equilibrium. Thus, one must be able to make a well-defined, stable, electrical contact to the polymer gate. This contact is not easy with most polymers, although adequate contacts to achieve rectifying polymer diodes have recently been fabricated (34-36).

Other technical considerations in designing a specific gas-sensitive polymer include the degree of specificity and the possibility of poisoning. In other words, will the polymer be specifically absorbing for one and only one molecule, or can other gaseous species interfere and give false alarms? Conversely, can the device as a whole be poisoned and rendered useless by the presence of a different gaseous agent? These problems must be considered in the initial polymer design phase, and we shall assume they have been solved in the following discussion of sensitivity and related parameters.

A hydrogen-sensitive FET (refer to the section on the "General Theory of Chemically Sensitive Field-Effect Transistors") has recently been demonstrated (5). This device uses a palladium metal gate to absorb gaseous hydrogen in concentrations as low as a few parts per million (ppm). The absorbed hydrogen appears to change the palladium work function, but the actual mechanism of this change is still debatable.

Feasibility of the Work-Function Dependent CHEMFET

In the following calculations, when the gas agent ionizes in the polymer, the agent is assumed to donate an electron to the conduction band of the polymer. All of the following arguments hold true if the opposite effect happens--that is, if holes are added to the valence band rather than electrons to the conduction band; and, in such a case, the Fermi level is shifted by a negative amount rather than a positive amount.

The cross-section of a possible device geometry is shown in Figure 17. For this device to work, the gate must be referenced to a well-defined potential; therefore, an ohmic contact must be made between the gate material and the transistor substrate. In general, ohmic contact to conducting polymers is not easy to achieve, and will depend critically on the particular materials involved. Preliminary research that electrically characterizes the gate materials will have to be done before the working devices are fabricated. The detailed band structure involved in these types of contacts is discussed elsewhere (37).

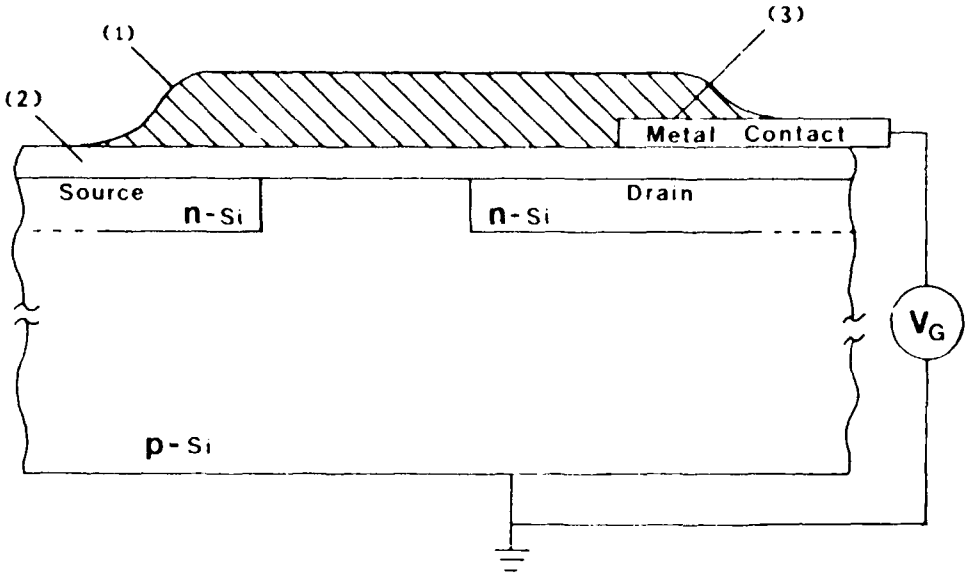

Figure 17. Structure of the work-function dependent field-effect transistor. [1 = organic polymer; 2 = insulator; and 3 = gate metal contact.]

The concentrations of all species will be in number per cubic centimeter. Thus, a concentration of 3 parts per billion (ppb) for a gas agent corresponds to approximately 10^{11} molecules/cm^3. The concentration of molecules of gas agent in the polymer, C_p, in equilibrium with the concentration of molecules of gas agent in the air, C_a, is given by:

$$C_p = \alpha C_a \tag{40}$$

in which α is the solubility coefficient. Further, the concentration of nonionized gas agent molecules in the polymer must eventually reach equilibrium with the concentration of ionized gas molecules. Assuming that the gas agent becomes singly ionized:

$$C_p \rightleftharpoons C_p^+ + e^- \tag{41}$$

where e^- is the electron donated to the conduction band.

In equilibrium, a dissociation constant exists for the reaction described in Equation 41:

$$K = \frac{[C^+]\,[e^-]}{[C_p]} \tag{42}$$

or

$$K = \frac{n_e^2}{\alpha C_a} \tag{43}$$

where n_e is the concentration of electrons donated to the conduction band from Equation 41.

For the semiconducting polymer:

$$n = n_o + n_e \tag{44}$$

in which n is the total concentration of electrons in the conduction band; n_o is the concentration of electrons which would exist in the conduction band with no gas agent present; and n_e is the additional concentration of electrons donated to the conduction band due to the presence of the gas agent.

The Fermi level, E_F, of the semiconductor can be written in terms of the intrinsic Fermi level (when the concentration of electrons equals the concentration of holes), E_i, and the actual concentration of electrons, n, and holes, p, in the material:

$$E_f = E_i + \frac{kT}{2} \ln \frac{n}{p} \tag{45}$$

or, equivalently:

$$E_f = E_i + \frac{kT}{2} \ln n^2 + \text{constant} \tag{46}$$

in which k is Boltzmann's constant and T is absolute temperature (°K).

Thus, changes in the Fermi level can be written as

$$\Delta E_f = kT \frac{\Delta n}{n} \tag{47}$$

Changes in the drain current of a field-effect transistor can readily be measured for gate voltage (or work-function) shifts of 25 millivolts (mV). Assuming that the Fermi level shifts by 25 mV, the required magnitude of the dissociation constant, K, can be calculated. Equations 43 and 47 become:

$$\frac{n_e}{n_o} = 1 = \frac{(K \alpha C_a)^{1/2}}{n_o} \tag{48}$$

or

$$K = \frac{n_o^2}{\alpha C_a} \tag{49}$$

Assuming the solubility coefficient, α, to be near unity, and C_a to be 10^{11} cm^{-3} (3 ppb), K can be estimated for different values of n_o. A semiconducting polymer has been reported (35) with n_o as small as 10^{10}, although a commonly attainable value would be a few orders of magnitude larger.

If n_o were 10^{10}, then $K = 10^9$; for a realistic maximum, if n_o were 10^{15}, then $K = 10^{19}$. Neither of these numbers are unreasonably large, but their attainability depends crucially on the polymer engineering of the semiconductor.

As already shown in Equation 19, the drain current, I_D, for a MOSFET is:

$$I_D = \frac{W}{L} \mu_n C_o \left[(V_G - V_T) V_D - \frac{V_D^2}{2}\right] \tag{50}$$

The prefactors are parameters of device geometry, substrate, and insulator materials. The threshold voltage is given by:

$$V_T = \phi_{ms} - \frac{Q_{ss}}{C_o} + 2\phi_F - \frac{Q_B}{C_o} - \frac{1}{C_o} \int_o^d \frac{x}{d} \rho(x)\, dx \qquad (51)$$

The term ϕ_{ms} is the work-function (of Fermi level) difference between the gate material and the semiconductor substrate material. This term must have a dynamic range. With proper ion-implanted channel, Equation 50, when an appropriate range of drain voltages is considered, reduces to:

$$I_D = p\,(V_G - V_T) \qquad (52)$$

in which p is a parameter accounting for the device geometry except for the gate. Thus, over a wide range of operating parameters, the device exhibits a linear response to changes in the threshold voltage and, therefore, in the work function.

CONCLUSIONS

Of the four types of CHEMFETs discussed in this report, only two currently have a chance to meet the CW agent detector specifications: the work-function CHEMFET, and the galvanostatic CHEMFET.

The work-function CHEMFET seems to be the optimum candidate, but cannot be thus designated until the electrical properties of the CW agent reactive polymer have been determined. To obtain a 25 mV signal for a 3 ppb concentration of gaseous CW agent, the intrinsic electron density, n_o, must be on the order of 10^{10} with a binding constant, $K = 10^9$. These are not unreasonable membrane requirements for the present conducting polymers.

The galvanostatic CHEMFET is the second candidate. To realize this type of sensor, the electrical characteristics of the polymer must be determined as well as the solid-state electrochemistry of the CW agents. (Since these facts are unknown to us, the feasibility of this device is rated significantly below that of the previous type of sensor.)

Our overall recommendation, at this time, is that the electrical properties and binding characteristics of the candidate polymers be evaluated before consideration is given to fabricating CW agent detector CHEMFETs.

REFERENCES CITED

1. Owen, D. R., and J. Jacobus. USAF School of Aerospace Medicine, Aerospace Medical Division, AFSC, Southeastern Center for Electrical Engineering Education, (SCEEE) Contract F33615-78D-0617-0012, Resin polymers for filtering and sensing of chemical agents, Tulane U., 1 Dec 1978 - 30 July 1979.

2. Grove, A. S. Physics and technology of semiconductor devices. New York: Wiley, 1967.

3. Many, A., Y. Goldstein, and N. B. Grover. Semiconductor surfaces. Amsterdam: North Holland Publ. Co., 1965.

4. Janata, J., and S. D. Moss. Chemically sensitive field-effect transistor. Biomed Eng 11:241 (1967).

5. Lundstrom, I., et al. A hydrogen-sensitive MOS field-effect transistor. Appl Phys Lett 26:55 (1975).

6. Lewis, F. A. The palladium hydrogen system. New York: Academic Press, 1967.

7. Lundstrom, I. and T. DiStefano. Influence of hydrogen on platinum-silicon dioxide-silicon structures. Surf Sci 59:23 (1976).

8. Bergveld, P., et al. Physical mechanisms for chemically sensitive semiconductor devices. Nature 273:438 (1978).

9. Lundstrom, I. Chemical reaction on Pd-surfaces studied with a Pd-MOS. Surf Sci 64:497 (1977).

10. Chauvet, F., and P. Caratge. A palladium MOS transistor for hydrogen detector applications. Acad Sci Ser B 285:153 (1977).

11. Lundstrom, I., et al. Hydrogen in smoke detected by the Pd-gate field-effect transistor. Rev Sci Instrum 47:738 (1976).

12. Shivaraman, M. S. Detection of H_2S with Pd-gate MOS field effect transistors. J Appl Phys 47:3592 (1976).

13. Lundstrom, I., et al. Hydrogen-sensitive Pd-gate MOS transistor. J Appl Phys 46:3876 (1975).

14. Kelly, R. G. Microelectronic approaches to solid-state ion selective electrodes. Electrochim Acta 22:1 (1977).

15. Buck, R. P., and D. E. Hackleman. Field effect potentiometric sensors. Anal Chem 49:2315 (1977).

16. Janata, J. Part I: Thermodynamics of chemically sensitive field effect transistors, p. 41. In P. Cheung (ed). Theory, design, and biomedical applications of solid-state chemical sensors. West Palm Beach, Fla.: CRC Press, Inc., 1978.

REFERENCES CITED (Cont'd.)

17. Zemel, J. N. Ion-sensitive field effect transistors and related devices. Anal Chem 47:255A (1975).

18. Bergveld, P. Development of an ion-sensitive solid-state device for neurophysiological measurements. IEEE Trans Biomed Eng, BME-17:70 (1970).

19. Bergveld, P. Development, operation, and application of the ion-sensitive field-effect transistor as a tool for electrophysiology. IEEE Trans Biomed Eng, BME-19:342 (1972).

20. Zemel, J. N. Chemically-sensitive semiconductor devices. Research and Development 28:38 (1977).

21. Revesz, A. G. On the mechanism of the ion-sensitive field effect transistor. Thin Solid Films 41:L43 (1977).

22. Moss, S. D., et al. Potassium ion-sensitive field effect transistor. Anal Chem 47:2238 (1975).

23. Moss, S. D., et al. Hydrogen, calcium, and potassium ion-sensitive FET transducers: A preliminary report. IEEE Trans Biomed Eng, BME-25:49 (1978).

24. Moss, S. D., et al. A microelectrode pH sensor. J Bioeng 1:11 (1977).

25. Storp, P., and G. G. Guilbault. A new assay for cholinesterase potentiometric determinations in flow streams. Anal Chim Acta (Amsterdam) 62:425 (1972).

26. Baum, G., and F. B. Ward. General enzyme studies with a substrate-selective electrode: Characterization of cholinesterases. Anal Biochem 42:487 (1971).

27. Crochet, K. L., and J. G. Mantalvo. Enzyme electrode system for assay of serum cholinesterase. Anal Chim Acta (Amsterdam) 66:259 (1973).

28. Gibson, K., and G. G. Guilbault. A potentiometric assay of cholinesterase. Anal Chim Acta (Amsterdam) 76:245 (1975).

29. Baum, G. An automated kinetic analysis of cholinesterase activity by a substrate-selective ion-exchange electrode, p. 193. In M. Kessler et al. (eds.). Ion and enzyme electrodes in biology and medicine. Baltimore, Md.: University Park Press, 1976.

30. Johnson, C. C., et al. U.S. Patent 4,020,830: Selective sensitive apparatus, Mar 12, 1975, 40 pp.

31. Heyne, L., and D. Den Engelsen. The speed of response of solid electrolyte galvanic cells for gas sensing. J Electrochem Soc 124:727 (1977).

32. Racine, P., and W. Mindt. Role of substrate diffusion in enzyme electrodes. Experientia (Basel) Suppl 18:525 (1971).

33. Goodings, E. P. Conductivity and superconductivity in polymers. Chem Soc Rev 5:95 (1976).

34. Fan, Fu-Ren, and L. R. Faulkner. Photovoltaic effects of metalfree and zinc phthalocyanines: I. Dark electrical properties of rectifying cells. J Chem Phys 69:3334, 3342 (1978).

35. Epstein, A. J., and J. S. Miller. Linear-chain conductors. Sci Am 241:52 (1979).

36. Fan, Fu-Ren, and L. R. Faulkner. Phthalocyanine thin films as semiconductor electrodes. J Am Chem Soc 101:4779 (1979).

37. Sze, S. M. Physics of semiconductor devices, New York: Wiley-Interscience, 1969.

SUPPLEMENTARY REFERENCES

Bergveld, P. Ion sensitive field effect transistors, p. 299. Proc. Int'l. Conf. on Biomed. Transducers, Paris, 3-7 Nov 1975. Paris, France: Electronics Industries Assoc., 1975.

Bergveld, P., J. Wiersma, and H. Meerteens. Extracellular potential recordings by means of a field effect transistor without gate metal, called OSFET. IEEE Trans Biomed Eng, BME-23:136 (1976).

Bowers, L. D., and P. W. Carr. Applications of immobilized enzymes in analytical chemistry. Anal Chem 48:544A (1967).

Buck, R. P. Theory of potential distribution and response of solid state membrane electrodes. Anal Chem 40:1432 (1968).

Buck, R. P., and V. R. Shepard. Reversible metal/salt interfaces and the relation of second kind and "all-solid-state" membrane electrodes. Anal Chem 46:2097 (1974).

Carmack, G. D., and H. Freiser. Electrical charge conduction mechanism in polymer membrane ion selective electrodes. Anal Chem 47:2249 (1975).

Cheung, P. W., et al. Theory, design, and biomedical applications of solid state chemical sensors. West Palm Beach, Fla.: CRC Press Inc., 1978.

Comte, P. A., and J. Janata. A field effect transistor as a solid-state reference electrode. Anal Chim Acta (Amsterdam) 101:247 (1978).

Esashi, M., and T. Matsuo. Integrated micro multi ion sensor using field effect of semiconductor. IEEE Trans Biomed Eng, BME-25:184 (1978).

SUPPLEMENTARY REFERENCES (Cont'd.)

Janata, J., S. D. Moss, and C. C. Johnson. Ion selective field effect transistor, p. 305. Proc. Int'l. Conf. on Biomed. Transducers, Paris, 3 - 7 Nov 1975. Paris, France: Electronics Industries Assoc., 1975.

Kneebone, B. M., and H. Freiser. Determination of nitrogen oxides in ambient air using a coated-wire nitrate ion selective electrode. Anal Chem 45:449 (1973).

Matsuo, T., and K. Wise. An integrated field-effect electrode for biopotential recording. IEEE Trans Biomed Eng, BME-21:485 (1974).

McMillan, R. E., and R. P. Misra. Insulating materials for semiconductor surfaces. IEEE Trans on Electrical Insulation, EI-5:10 (1970).

Revesz, A. G., and K. H. Zaininger. The Si-SiO_2 solid-solid interface system. RCA Review 29:22 (1968).

Schenck, J. F. A transistor method for measuring changes in double layer potentials. J Colloid and Interface Science 61:569 (1977).

Schlegel, E. S., et al. Behavior of surface ions on semiconductor devices. IEEE Trans on Electron Devices, ED-15:973 (1968).

Schmidt, P. F. Electronic interaction between impurities in the oxide film and the semiconductor substrate. IEEE Trans on Electron Devices, ED-12:102 (1965).

Senturia, S. D., C. M. Sechen, and J. A. Wishneusky. The charge-flow transistor: A new MOS device. Appl Phys Lett 30:106 (1977).

Steele, M. C., and B. A. MacIver. Palladium/cadmium-sulfide Schottky diodes for hydrogen detection. Appl Phys Lett 28:687 (1976).

Stiblert, L., and C. Svensson. Hydrogen leak detector using a Pd-gate MOS transistor. Rev Sci Instrum 46:1206 (1975).

Szedon, J. R., and J. P. Stelmak. Effects of organic and inorganic dielectric films on semiconductor devices. IEEE Trans on Electrical Insulation, EI-5:3 (1970).

Watson, J., and A. Price. Selectivity of semiconductor gas sensors. Proc IEEE 66:1670 (1978).

Wise, J. C. M., and A. Davies. A simple sulphur-dioxide meter. Med Biol Eng (Oxford) 14:545 (1976).

ABBREVIATIONS, ACRONYMS, AND SYMBOLS

CHEMFETs	chemically sensitive field-effect transistors
CSSD	chemically sensitive semiconductor devices
CW	chemical warfare
FET	field-effect transistor
IGFET	insulated-gate field-effect transistor
ISA	ion-sensitive electrode
ISFET	ion-sensitive field-effect transistor
mA	milliampere
MIS	metal-insulator-semiconductor
MOS	metal-oxide semiconductor
MOSFET	metal-oxide-semiconductor field-effect transistor
mV	millivolt
Pd	palladium
ppb	parts per billion
ppm	parts per million
Si	silicon
SiO_2	silicon dioxide
V	voltage

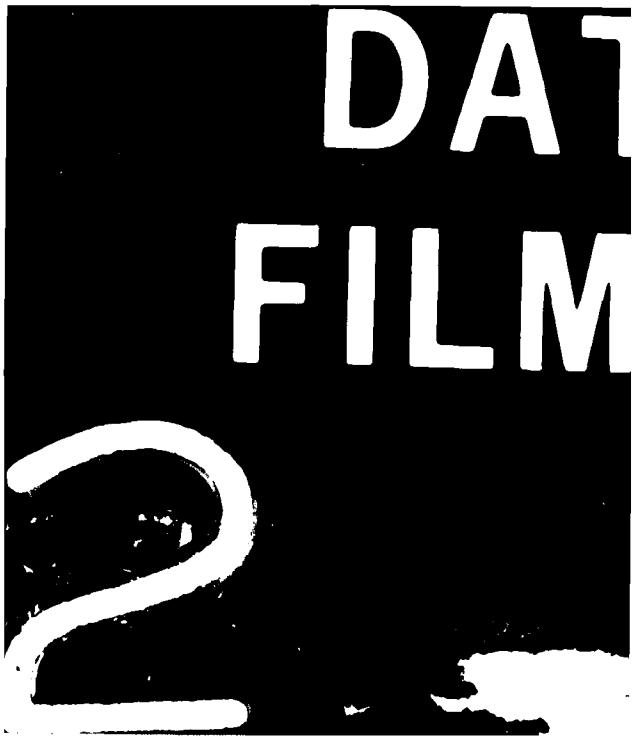
DAT
FILM